# 7. Bulk electrolysis (ch. 11)

**Learning subject**

1. Classifications of bulk electrolysis
2. General considerations in bulk electrolysis
3. Controlled-potential methods
4. Controlled-current methods
5. Electrometric end-point detection
6. Flow electrolysis
7. Thin-layer electrochemistry
8. Stripping analysis

A.J. Bard, L. R. Faulkner, Electrochemical Methods, Wiley, 2001.

# (Bulk) electrolysis

A small ratio of electrode area(A) to solution volume(V) (previous Chapters or typical electrochemistry) → long time period for the product in solution (e.g. O + e → R)

e.g. 5 x $10^{-4}$ M O species in solution with V = 100 $cm^3$ and A = 0.1 $cm^2$ → 100 μA(current density 1 $mA/cm^2$) for 1 h → 0.36 C electricity, so 1% change in solution

Circumstances where one desire to alter the composition of the bulk solution → "electrolysis"

(Bulk) electrolysis: analytical measurements, removal or separation of solution components, electroysnthesis

Bulk electrolysis: large A/V conditions, effective mass-transfer conditions
e.g. e.g. 5 x $10^{-4}$ M O species in solution with V = 100 $cm^3$ and A = 100 $cm^2$ → 0.1 A(current density 1 $mA/cm^2$) for 1 h → 10 min change completely in solution

**Table 15.1.** Industrial electrolysis and electrosynthesis

| | |
|---|---|
| Chlor-alkali industry[9–13] | Extraction of chlorine and sodium hydroxide from NaCl |
| Metal extraction | Aluminium (Hall–Heroult process)[14–16]<br>Sodium, magnesium, lithium (electrolysis of the fused salts)<br>Electrolysis in aqueous solution (principally copper and zinc) |
| Electrolysis in the preparation of inorganic compounds[17] | Strong oxidizing agents: $KMnO_4$, $K_2Cr_2O_7$, $Na_2S_2O_8$, $F_2$, $NaClO_3$.<br>Active metal oxides: $MnO_2$, $Cu_2O$<br>Hydrogen and oxygen by water electrolysis[18–20] |
| Electro-organic synthesis[21–24]<br>(Ch. 12) | Hydrodimerization of acrylonitrile (Monsanto process)<br>Direct processes e.g. reduction<br>$Me_2CO \rightarrow$ i-PrOH<br>Indirect processes—an inorganic reagent is used as catalyst, being oxidized or reduced at the electrode to give a species that reacts with the organic compound e.g.<br>Electrode(Pb): $Cr^{3+} \rightarrow Cr_2O_7^{2-}$<br>Solution: $Cr_2O_7^{2-}$ + anthracene → anthraquinone + $Cr^{3+}$ |

C. M. A. Brett, A. M. O. Brett, Electrochemistry, Oxford, 1994.

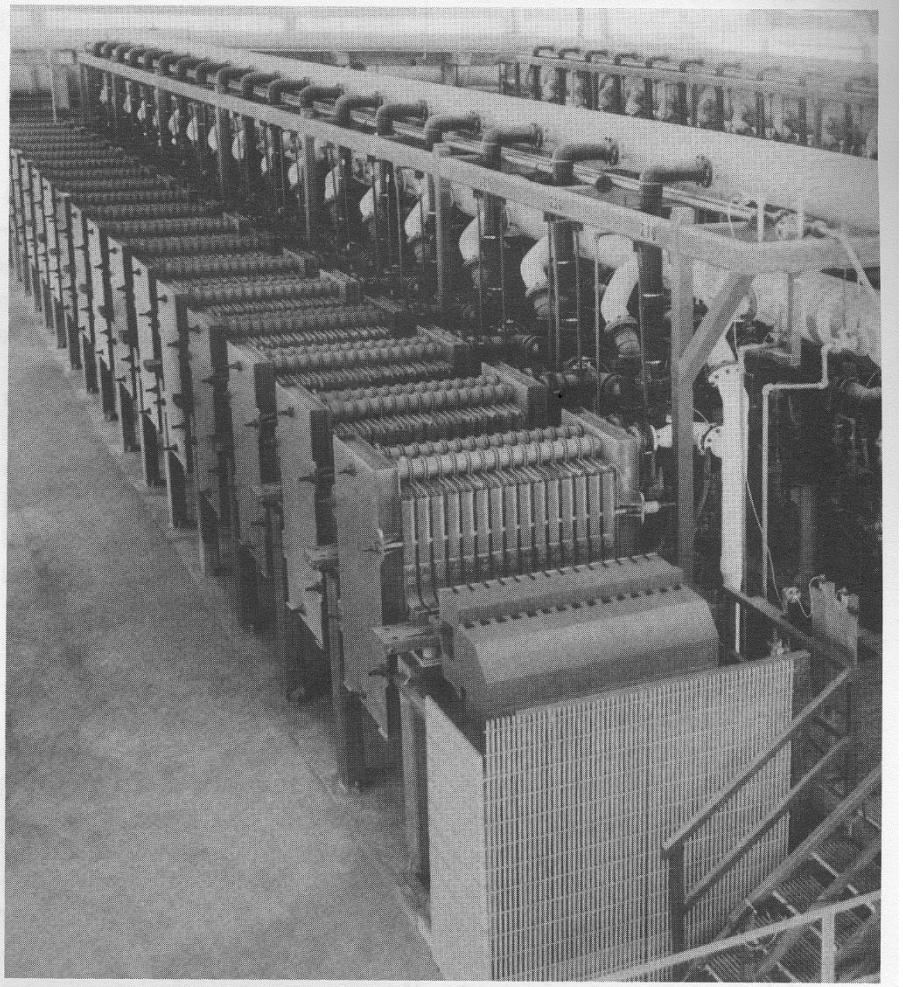

Figure I. A Modern Chlor-Alkali Cell Installation Using Ion Exchange Membrane Cells. Each electrolyzer consists of a number of planar cell elements separated from each other by a sheet of ion exchange membrane. Tie-rods and massive plates at either end of the electrolyzer hold the stacked structure in place. Two horizontal cylindrical tanks above each electrolyzer promote gas disengagement from the liquid electrolyte. The number of cell elements can be adjusted to accommodate currents up to 300,000 Amperes. Membrane cell plants producing up to 400 tons of chlorine, 440 tons of sodium hydroxide, and 5 million cubic feet of hydrogen per day have been built. Larger plants are expected in the near future as membrane cell technology matures. Improvements in the ion exchange membrane, electrodes, and cell design have lowered cell energy demand to 2100-2200 kwh per ton of sodium hydroxide.

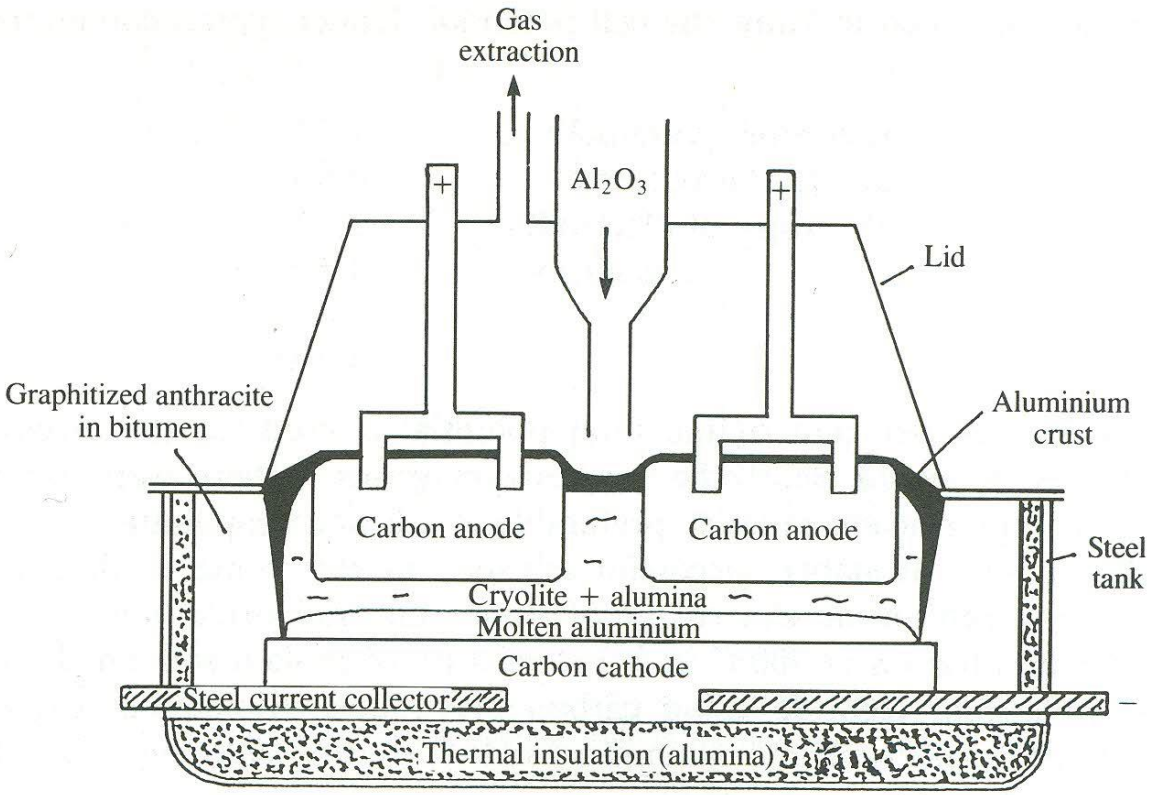


**Fig. 15.4.** Scheme of a cell for aluminium extraction by the Hall–Heroult process.

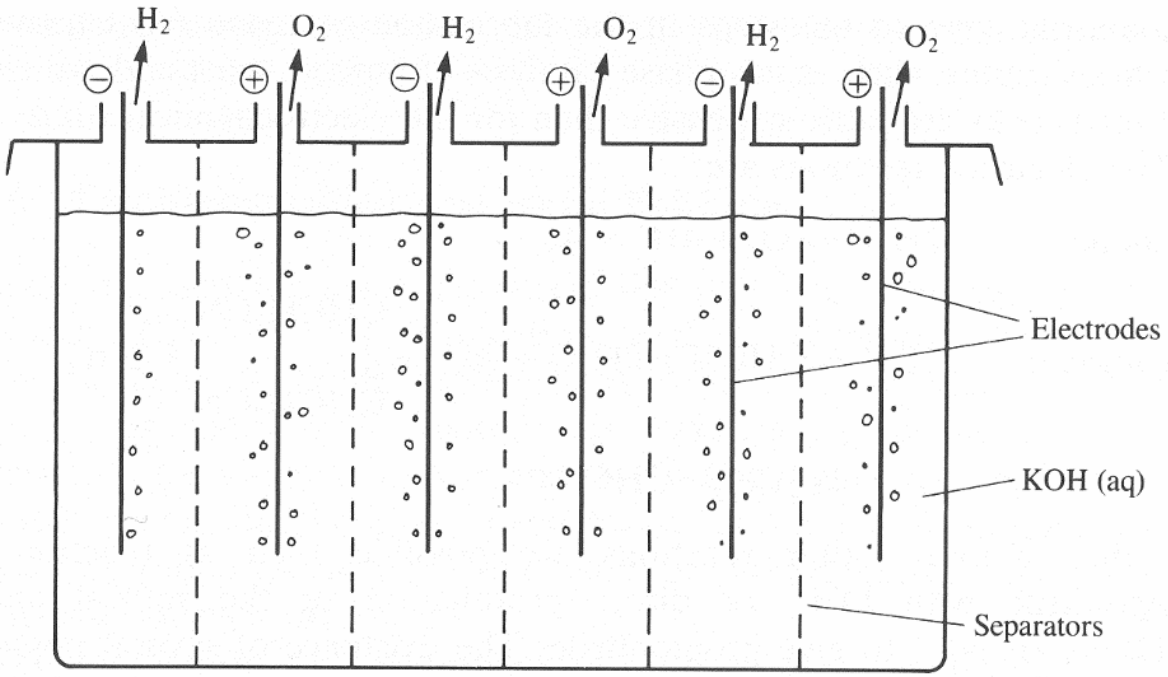


**Fig. 15.5.** Scheme of a cell for water electrolysis. Note the separators between the $H_2$ and $O_2$ produced. The electrical link is monopolar (but in other designs can be bipolar).

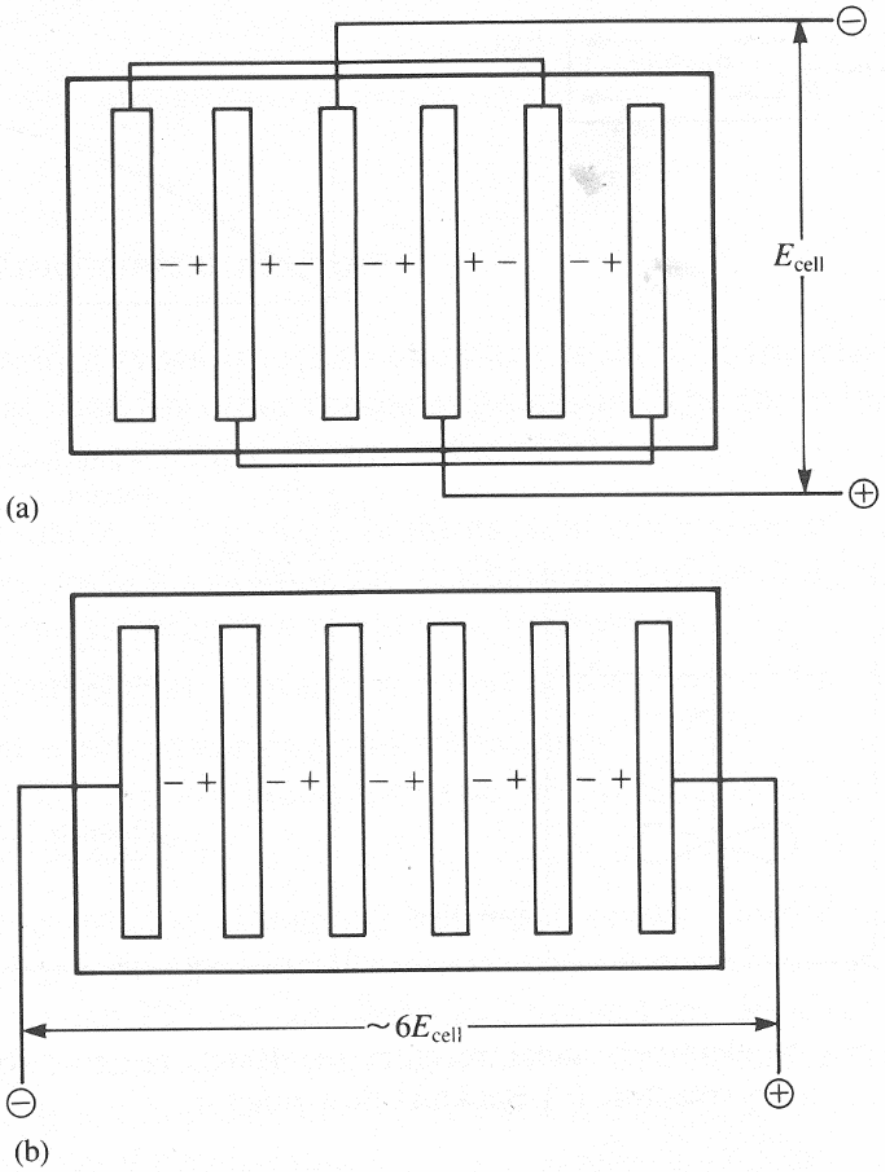


**15.2.** Scheme of multielectrode cells: (a) Monopolar; (b) Bipolar.

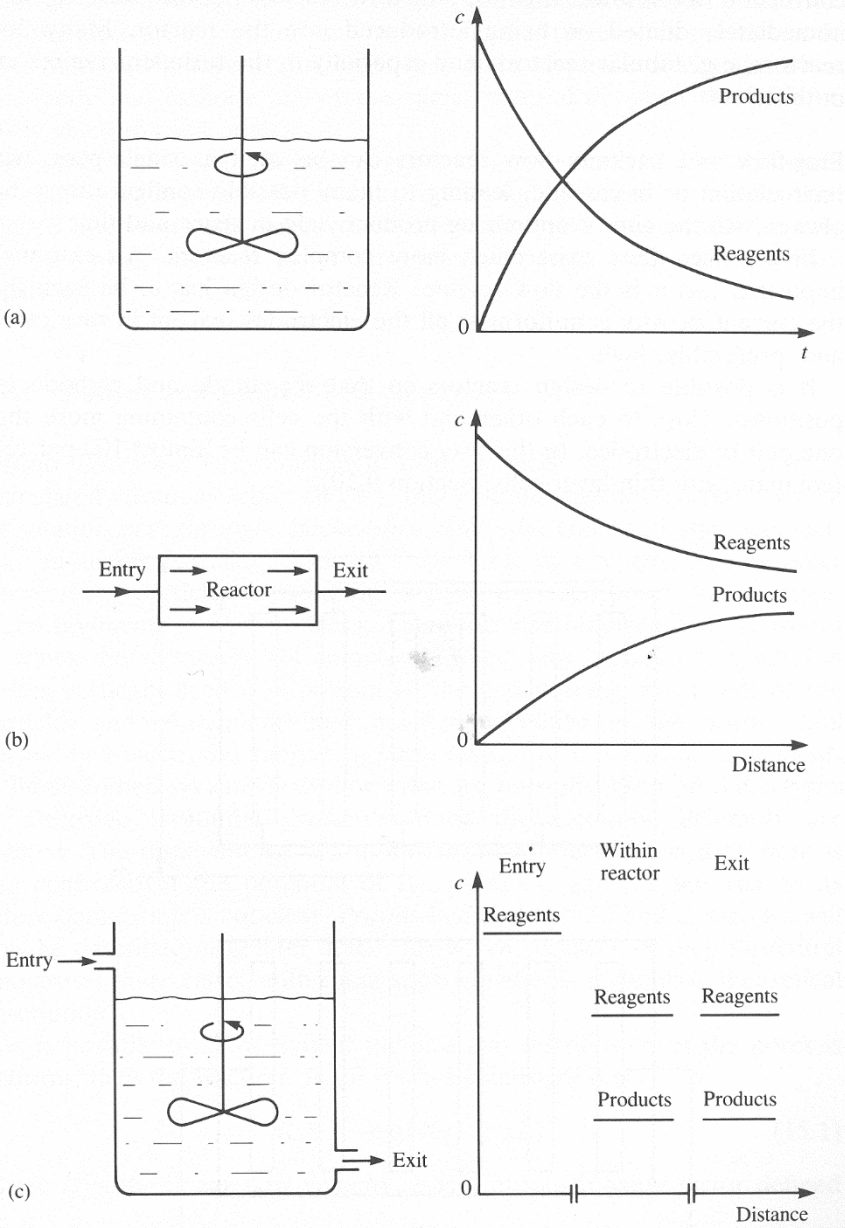


**Fig. 15.1.** Types of electrochemical reactor; (a) Batch reactor; (b) Plug flow reactor; (c) Backmix flow reactor.

# 1. Classification

(1) Controlled parameter (E or i)
(i) Controlled-potential techniques

(ii) Controlled-current techniques

(2) Purpose
Electrogravimetry

Coulometry

Electroseparation

(3) Related bulk electrolysis techniques

Thin-layer electrochemical methods: large A/V ratios, but small volume of a solution in a thin layer (20~100 μm)

Flow electrolysis

Stripping analysis

# 2. General considerations in bulk electrolysis

(1) Extent or completeness of an electrode process
The extent or degree of completion of a bulk electrolytic process can be predicted for nernstian reactions

(a) Both forms soluble in solution

$$O + ne \rightleftarrows R$$

$$E = E^{0'} + \left(\frac{RT}{nF}\right) \ln\left(\frac{C_O}{C_R}\right)$$

where both O and R are soluble and R is initially absent.

Let $C_i$: initial concentration of O, $V_s$: volume of the solution, x: fraction of O reduced to R at the potential E

$$\text{moles O at equilibrium} = V_s C_i (1 - x)$$
$$\text{moles R at equilibrium} = V_s C_i x$$

$$\boxed{E = E^{0'} + \left(\frac{RT}{nF}\right) \ln\left[\frac{(1 - x)}{x}\right]}$$

or

$$\text{fraction of O reduced} = x = \{1 + 10^{[(E-E^{0'})n/0.059]}\}^{-1} \text{ (at 25°C)}$$

e.g. 99% completeness of reduction of O to R (i.e. x = 0.99), the potential of the working electrode should be

$$E = E^{0'} + \frac{0.059}{n} \log\left(\frac{0.01}{0.99}\right) \approx E^{0'} - \frac{(0.059)(2)}{n}$$

or 118/n mV more negative than $E^{0'}$ at 25℃

(b) Deposition as an amalgam

$$O + ne \overset{Hg}{\rightleftarrows} R(Hg)$$

R dissolved in a (mercury(Hg)) electrode of volume $V_{Hg}$

$$E = E_a^{0'} + \frac{RT}{nF} \ln\left[\frac{(V_s C_i (1-x)/V_s)}{(V_s C_i x/V_{Hg})}\right]$$

$$E = E_a^{0'} + \frac{RT}{nF} \ln\left(\frac{V_{Hg}}{V_s}\right) + \frac{RT}{nF} \ln \frac{1-x}{x}$$

(c) Deposition of a solid

$$O + ne \rightleftharpoons R \text{ (solid)}$$

when more than a monolayer of R is deposited on an inert electrode (e.g. Cu electrodeposition on Pt, Cu deposition on Cu). The activity of R, $a_R$, is constant and equal to unity

$$E = E^0 + \frac{RT}{nF} \ln[\gamma_O C_i (1 - x)]$$

where $\gamma_0$: the activity coefficient of O. When less than a monolayer of R is deposited, $a_R \neq 1$, and $a_R$ is a function of coverage ($\theta$)

$$a_R \approx \gamma_R \theta = \gamma_R \frac{A_R}{A} = \frac{\gamma_R N_R A_a}{A}$$

A: the electrode area, $A_R$: area occupied by R, $A_a$: the cross-sectional area of a molecule of R, $N_R$: the number of molecules of R deposited on the electrode.

At equilibrium

$$N_R = V_s C_i x N_A$$

So the Nernst equation

$$E = E^0 + \frac{RT}{nF} \ln\left(\frac{\gamma_O A}{\gamma_R V_s N_A A_a}\right) + \frac{RT}{nF} \ln\left(\frac{1 - x}{x}\right) \qquad (11.2.15)$$

# The shape of the deposition curve

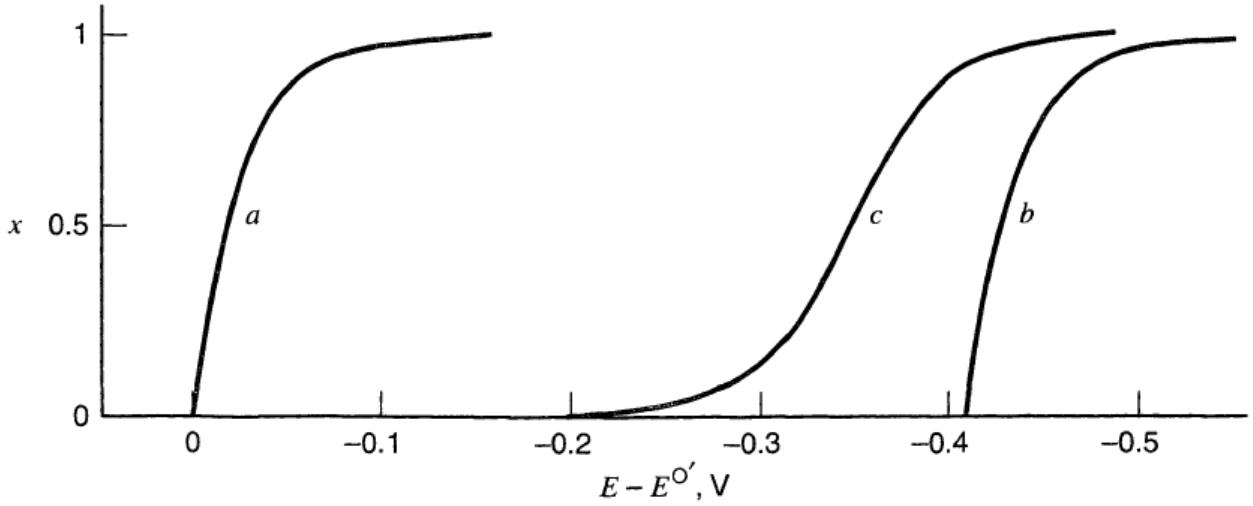


**Figure 11.2.1** Fraction of a metal $M^+$ (e.g., $Ag^+$) deposited ($x$) as a function of potential. *Curve a*: 1 *M* $Ag^+$ on Ag. *Curve b*: $10^{-7}$ *M* $Ag^+$ on Ag. *Curve c*: $10^{-7}$ *M* $Ag^+$ on Pt, according to (11.2.15).

The deposition begins at potentials more positive than values where deposition of R occurs on bulk R.

e.g. Ag on 1 $cm^2$ Pt electrode from 0.01 L solution containing $10^{-7}$ M $Ag^+$. Let $A_a$ = 1.6 x $10^{-16}$ $cm^2$ and $\gamma_O = \gamma_R \rightarrow$ the potential for deposition of one-half of the silver (~0.05 monolayer) is E = 0.35 V, compared to E = 0.43 V required for the same amount of deposition on a Ag electrode. Deposition at potentials before that predicted by the Nernst equation with $a_R = 1$ is called underpotential deposition.

Slow e-transfer (irreversible) process: more negative potential, catalyst needed

(2) Current efficiency

The fraction of the total current

$$\text{Instantaneous current efficiency for } r\text{th process} = i_r/i_{total}$$

A current efficiency of unity (or 100%) = only one process is occurring at an electrode

An electrolysis over some period of time

$$\text{Overall current efficiency for } r\text{th process} = Q_r/Q_{total}$$

High current efficiency desirable: electrode potential chosen at no side reactions (e.g. reduction or oxidation of solvent, supporting electrolyte, electrode materials, or impurities)

# (3) Electrolysis cells

## Bulk electrolysis: longer duration & larger current → cell design is important

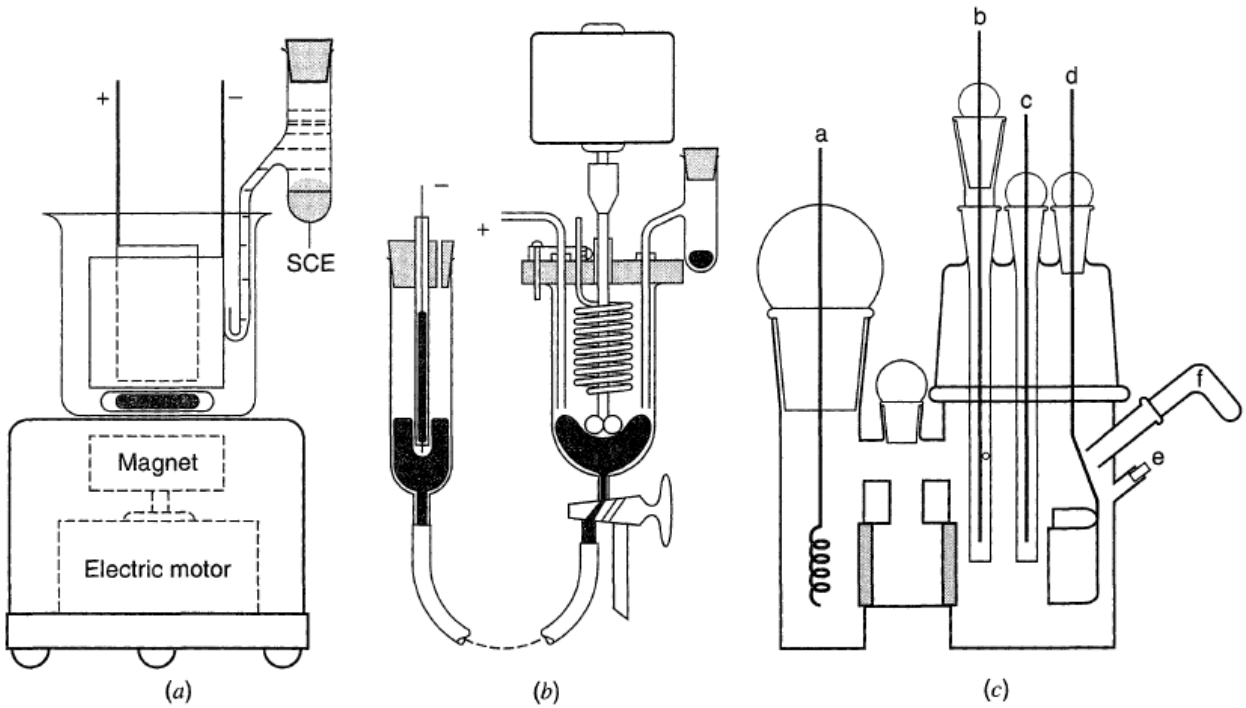


**Figure 11.2.2** Typical cells for bulk electrolysis. (*a*) Undivided cell for controlled-potential separations and electrogravimetric analysis at a solid cathode. [From J. J. Lingane, *Anal Chim. Acta*, **2**, 584 (1948), with permission.] (*b*) Undivided cell for coulometric analysis at mercury cathode with a silver anode. [Reprinted with permission from J. J. Lingane, *J. Am. Chem. Soc.*, **67**, 1916 (1945). Copyright 1945, American Chemical Society.] (*c*) Three-compartment cell, with ground-glass joints, for coulometric and voltammetric studies on a vacuum line. (*a*) Platinum wire auxiliary electrode; (*b*) silver wire reference electrode in separate compartment; (*c*) gold voltammetric working microelectrode; (*d*) platinum foil coulometric working electrode; (*e*) silicone rubber septum for sample injection; (*f*) rotatable side arm for solid sample addition. Arm and joint for attachment of cell to the vacuum line are not shown. [Reprinted with permission from W. H. Smith and A. J. Bard, *J. Am. Chem. Soc.*, **97**, 5203 (1975). Copyright 1975, American Chemical Society.]

(a) Electrodes and geometry

Working electrodes for large area → wire gauzes, foil cylinders, packed beds of powders, slurries, fluidized beds, pools (of mercury)

Auxiliary(counter) electrodes are critical importance in bulk electrolysis cells : large area & symmetric with working electrode for uniform current density to prevent undesired side reactions

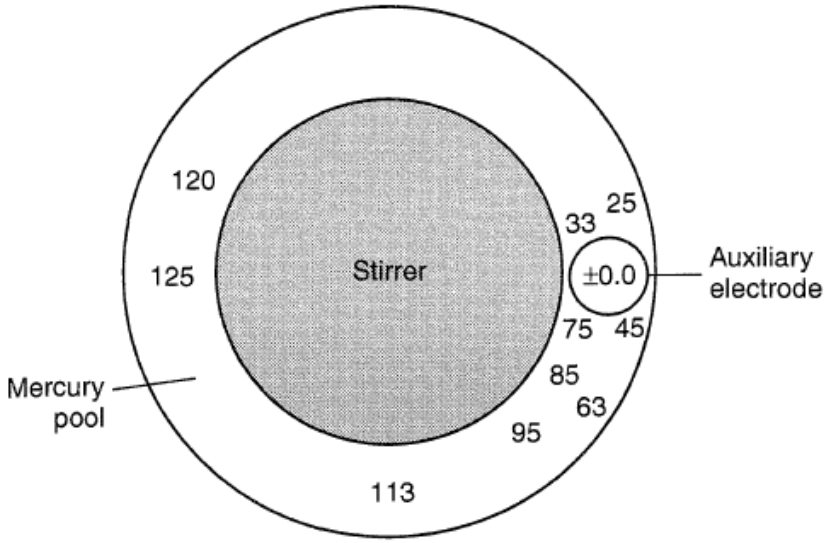


**Figure 11.2.3** Potential distribution in mV at surface of ring-shaped mercury pool electrode using an unsymmetrical auxiliary electrode. Solution: 0.5 *M* $H_2SO_4$; total cell current: 40 mA; pool: 1.5 in. o.d., 1.0 in. i.d. Small circle shows position of the auxiliary electrode's fritted-glass separator, situated 4 mm above the pool surface. [Reprinted with permission from G. L. Booman and W. B. Holbrook, *Anal. Chem.*, **35**, 1793 (1963). Copyright 1963, American Chemical Society.]

Reference electrode of a proper placement

(b) Separators

Soluble products may be reactive at the working electrode → separators between two electrodes: fritted glass disks, ion-exchange membrane, filter paper, asbestos mats, porous ceramics

Separators: no intermixing of anolyte and catholyte, low contribution to the cell resistance

(c) Cell resistance

Minimization of cell resistance in cell design is important → $iR^2$ waste power, high voltage output needed, undesirable heat evolution, more serious in nonaqueous solvents (due to lower dielectric constants, acetonitrile, N,N-dimethylformamide, tetrahydrofuran, ammonia etc)

# 3. Controlled-potential methods

(1) Current-time behavior $O + ne \rightleftarrows R$

Current-potential characteristics for stirred solutions: continuous decreasing $i_l$ as $C_O^*$ decreases during the electrolysis

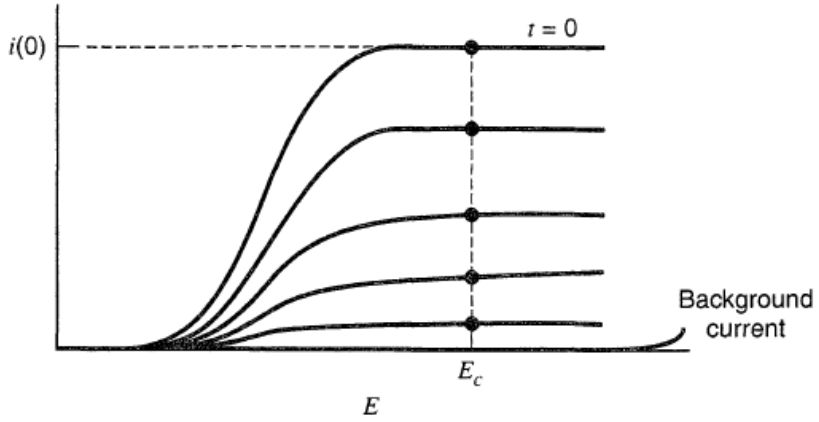


**Figure 11.3.1** Current-potential curves at different times during a controlled-potential bulk electrolysis at $E = E_c$.

Initially $C_O^*(0)$, electrode area A, potential in the limiting current region $E_c$, total number of moles of O $N_O$, total solution volume V

$$i_l(t) = nFAm_O C_O^*(t)$$

$$i_l(t) = -nF\left[\frac{dN_O(t)}{dt}\right] \qquad C_O^*(t) = \frac{N_O(t)}{V} \qquad i_l(t) = -nFV\left[\frac{dC_O^*(t)}{dt}\right]$$

$$\frac{dC_O^*(t)}{dt} = -\left(\frac{m_O A}{V}\right) C_O^*(t) = -pC_O^*(t) \qquad (11.3.5)$$

Initial condition $C_O^*(t) = C_O^*(0)$ at t = 0. Equation(11.3.5) is characteristic of a first-order, $p = m_0A/V$ is analogous to the first-order rate constant. The solution,

$$C_O^*(t) = C_O^*(0)\exp(-pt)$$

$$i(t) = i(0)\exp(-pt) \qquad (11.3.7)$$

A controlled-potential bulk electrolysis is like a first-order reaction

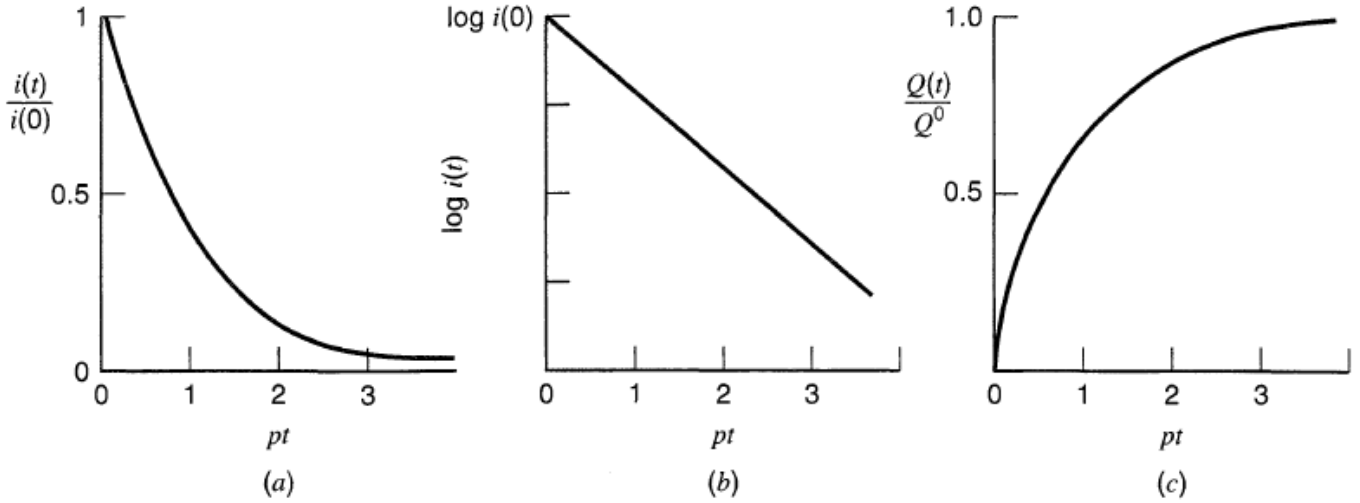


**Figure 11.3.2** (*a*) Current-time curve during controlled-potential electrolysis (in dimensionless form). (*b*) log $i(t)$ *vs. t.* (*c*) $Q$ *vs. t.*

Duration of the electrolysis (from (11.3.5))

$$\frac{-p}{2.3}t = \log\left[\frac{C_O^*(t)}{C_O^*(0)}\right] = \log\left[\frac{i(t)}{i(0)}\right]$$

For 99% completion of electrolysis, $C_O^*(t) / C_O^*(0) = 10^{-2}$, and $t = 4.6/p$; for 99.9% completion, $t = 6.9/p$. With effective stirring, $m_0 \sim 10^{-2}$ cm/s, so that for $A(cm^2) \sim V(cm^3)$, $p \sim 10^{-2}\ s^{-1}$, and a 99.9% electrolysis require ~690 s (~12 min). Typically 30~60 min

Total quantity of electricity Q(t) consumed in the electrolysis (Fig. 11.3.2c)

$$Q(t) = \int_0^t i(t)\,dt \qquad (11.3.9)$$

Controlled-potential is the most efficient method of carrying out a bulk electrolysis because the current is always maintained at the maximum value

## (2) Electrogravimetric methods

Determination of a metal by selective deposition on an electrode, followed by weighing

**TABLE 11.3.1 Deposition Potentials (V *vs.* SCE) for Various Metals in Different Media at a Platinum Electrode[a]**

| | Supporting Electrolyte | | | | |
|---|---|---|---|---|---|
| Metal | 0.2 *M* $H_2SO_4$ | 0.4 *M* NaTart + 0.1 *M* NaHTart | 1.2 *M* $NH_3$ + 0.2 *M* $NH_4Cl$ | 0.4 *M* KCN + 0.2 *M* KOH | EDTA + $NH_4OAc$[b] |
| Au | +0.70 | (+0.50)[d] | — | −1.00 | +0.40 |
| Hg | +0.40 | (+0.25)[d] | −0.05 | −0.80 | +0.30 |
| Ag | +0.40 | (+0.30)[b] | −0.05 | −0.80 | +0.30 |
| Cu | −0.05 | −0.30 | −0.45 | −1.55 | −0.60 |
| Bi | −0.08 | −0.35 | — | (−1.70)[d] | −0.60 |
| Sb | −0.33 | −0.75 | — | −1.25 | −0.70 |
| Sn[c] | — | — | — | — | — |
| Pb | — | −0.50 | — | — | −0.65 |
| Cd | −0.80 | −0.90 | −0.90 | −1.20 | −0.65 |
| Zn | — | −1.10 | −1.40 | −1.50 | — |
| Ni | — | — | −0.90 | — | — |
| Co | — | — | −0.85 | — | — |

[a] Adapted from table given in reference 3.

[b] 5 g $NH_4OAc$ + 200 mL $H_2O$ (pH ≈ 5); [EDTA]:[metal] = 3:1.

[c] Tin can be deposited from solutions of Sn(II) in HCl or HBr media.

[d] Metal deposits obtained are not suitable for electrogravimetric analysis.

# (3) Electroseparations

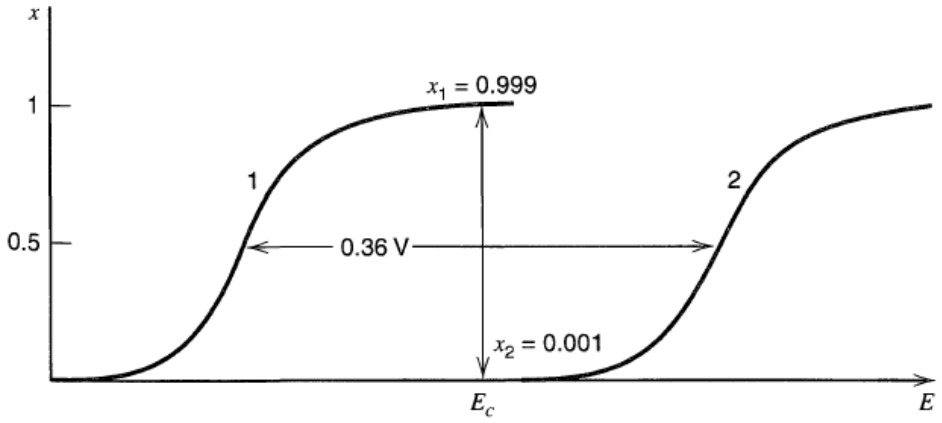


**Figure 11.3.3** Conditions for complete separation of metals $M_1$ and $M_2$ at a mercury electrode ($n_1 = n_2 = 1$).

| Ia | IIa | IIIa | IVa | Va | VIa | VIIa | VIII | | | 1b | IIb | IIIb | IVb | Vb | VIb | VIIb | 0 |
|---|---|---|---|---|---|---|---|---|---|---|---|---|---|---|---|---|---|
| H | | | | | | | | | | | | | | | | | He |
| Li | Be | | | | | | | | | | | B | C | N | O | F | Ne |
| Na | Mg | | | | | | | | | | | Al | Si | P | S | Cl | Ar |
| K | Ca | Sc | Ti | V | Cr | Mn | Fe | Co | Ni | Cu | Zn | Ga | Ge | As | Se | Br | Kr |
| Rb | Sr | Y | Zr | Nb | Mo | Tc | Ru | Rh | Pd | Ag | Cd | In | Sn | Sb | Te | I | Xe |
| Cs | Ba | La[a] | Hf | Ta | W | Re | Os | Ir | Pt | Au | Hg | Tl | Pb | Bi | Po | At | Rn |
| Fr | Ra | Ac[b] | | | | | | | | | | | | | | | |

Note: Heavy solid lines enclose elements that can be quantitatively deposited in the mercury cathode. Broken lines enclose elements that are quantitatively separated from the electrolyte, but are not quantitatively deposited in the mercury. Light lines enclose elements that are incompletely separated.
[a]Also elements 58 to 71 (partial deposition of lanthanum and neodymium has been reported).
[b]Also elements 90 to 103.

**Figure 11.3.4** Metals deposited at a mercury electrode. [Reprinted with permission from J. A. Maxwell and R. P. Graham, *Chem. Rev.*, **46**, 471 (1950). Copyright 1950, American Chemical Society.]

## (4) Coulometric measurements

In controlled-potential coulometry the total number of coulombs consumed in electrolysis is used to determine the amount of substance electrolyzed

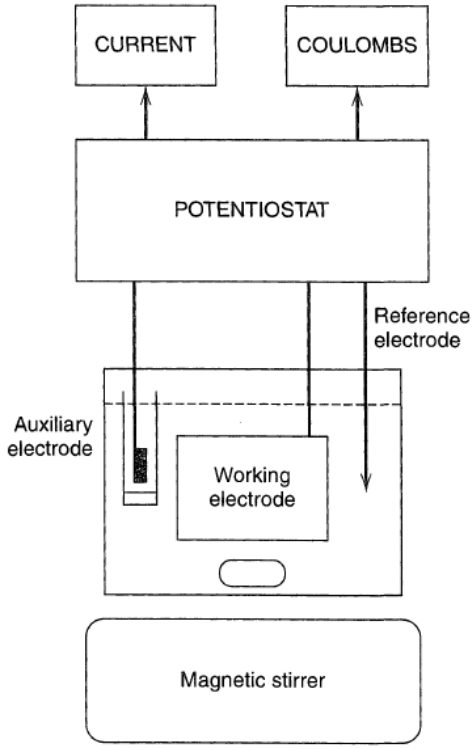


**Figure 11.3.5** Block diagram of typical controlled-potential coulometry apparatus.

Potential → i-t curve

→ Figure 11.3.2, Q-t. Equation (11.3.7) and (11.3.9)

$$Q(t) = \frac{i(0)}{p}(1 - e^{-pt}) = Q^0(1 - e^{-pt})$$

$$Q^0 = nFN_O = nFVC_O^*(0)$$ (11.3.11, Faraday's law)

where $Q^0$ at the completion of the electrolysis ($t = \infty$)

Numerous applications of controlled-potential coulometry (Table 11.3.2)

Controlled-potential coulometry is also a useful method for studying the mechanism of electrode reactions and for determining the n-value for an electrode reaction

$$O + e \rightleftharpoons R$$

$$R \rightarrow A \qquad \text{(slow, } t_{1/2} \sim 2\text{–}5 \text{ min)}$$

$$A + e \rightarrow B \qquad \text{(A reduced at less negative potentials than O)}$$

**TABLE 11.3.2 Typical Controlled-Potential Coulometric Determinations**

| Substance | Working Electrode | Supporting Electrolyte[a] | Control Potential (V *vs.* SCE) | Overall Reaction |
|---|---|---|---|---|
| Li | Hg | 0.1 *M* TBAP ($CH_3CN$) | −2.16 | Li(I) → Li(Hg) |
| Cr | Pt | 1 *M* $H_2SO_4$ | +0.50 | Cr(VI) → Cr(III) |
| Fe | Pt | 1 *M* $H_2SO_4$ | +0.20 | Fe(III) → Fe(II) |
| Zn | Hg | 2 *M* $NH_3$<br>1 *M* $(NH_4)_3$ Citrate | −1.45 | Zn(II) → Zn(Hg) |
| $Te^{2-}$ | Hg | 1 *M* NaOH | −0.60 | $Te^{2-} \rightarrow Te$ |
| $Br^-$ | Ag on Pt | 0.2 *M* $KNO_3$ (MeOH) | 0.0 | $Ag + Br^- \rightarrow AgBr$ |
| $I^-$ | Pt | 1 *M* $H_2SO_4$ | +0.70 | $2I^- \rightarrow I_2$ |
| U | Hg | 0.5 *M* $H_2SO_4$ | −0.325 | U(VI) → U(IV) |
| Pu | Pt | 1 *M* $H_2SO_4$ | +0.70 | Pu(III) → Pu(IV) |
| Ascorbic acid | Pt | 0.2 *M* phthalate buffer, pH 6 | +1.09 | Oxdn. $n = 2$ |
| DDT | Hg | | −1.60 | Redn. $n = 2$ |
| Aromatic hydrocarbons (e.g., diphenyl-anthracene) | Hg or Pt | 0.1 *M* TBAP (DMF) | | Redn. $Ar \rightarrow Ar^{\cdot-}$ |
| Aromatic nitro-compounds | Hg | 0.5 *M* LiCl (DMSO) | | Redn. $ArNO_2 \rightarrow ArNO_2^{\cdot-}$ |

[a]With water as solvent, unless indicated otherwise.

# 4. Controlled-current methods

## (1) Characteristics of controlled-current electrolysis

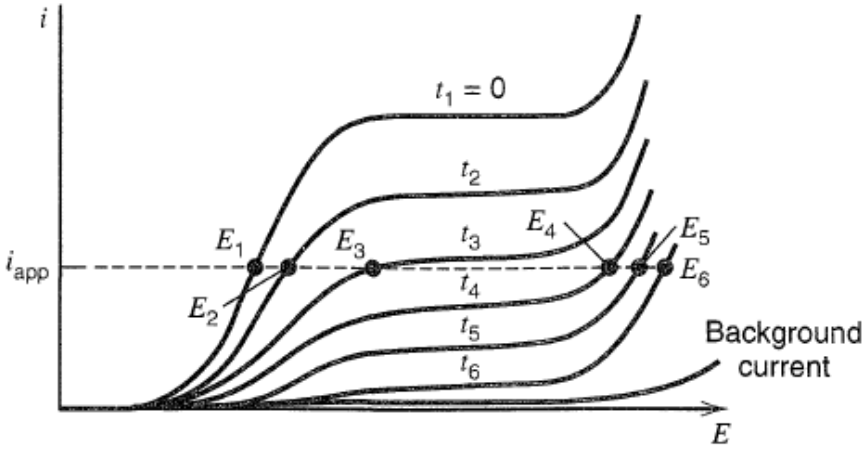


**Figure 11.4.1** Current-potential curves at different times (increasing from $t_1$ to $t_6$) during bulk electrolysis with an applied constant current, $i_{app}$. The electrode potential shifts from $E_1$ to $E_6$ during the course of the electrolysis, with the largest shift occurring (between curves *3* and *4*) when $i_{app} = i_l$.

$i_{appl} > i_l(t)$, as the electrolysis proceeds, $C_O^*(t)$ decreases and $i_l(t)$ decreases (linearly with time). When

$$C_O^*(t) = \frac{i_{app}}{nFAm_O}$$

$i_{appl} = i_l(t)$. At longer time, $i_{appl} > i_l(t)$, and the potential shifts to a new, more negative value, where an additional electrode reaction can occur; the current efficiency drops below 100% (potential is sufficiently negative)

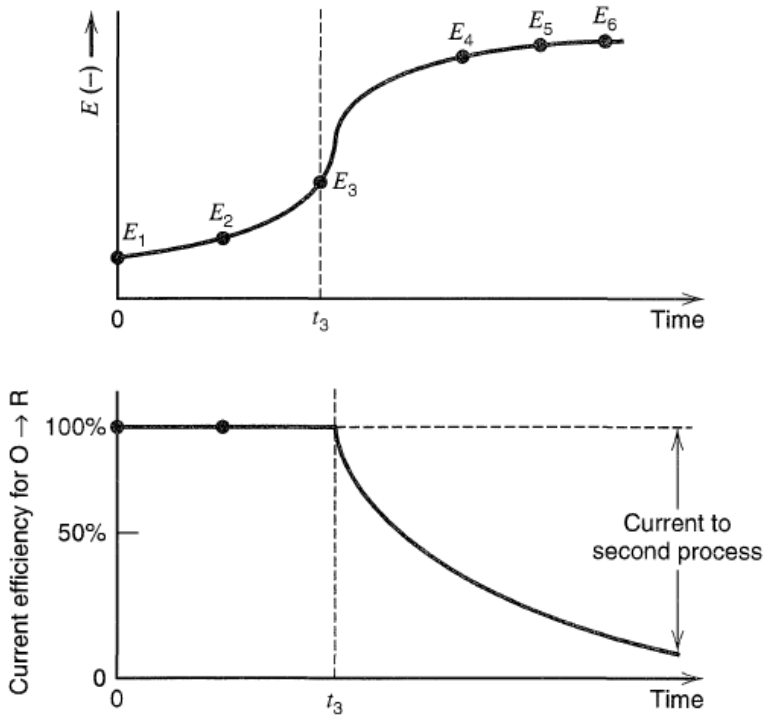


**Figure 11.4.2** Potential and current efficiency for the electrolysis illustrated in Figure 11.4.1.

(-)the selectivity of a controlled-current separation is intrinsically poorer than the corresponding controlled-potential method, since at some time during the electrolysis the potential must shift into a more negative region where a new electrode reaction occurs and, for example, a second metal could be deposited

(+)The simpler apparatus involved

Large-scale electrosynthesis or separations involving very high currents

Flow systems where the reactants are continuously added to the cell and products removed

## (2) Coulometric methods

A constant-current coulometric method is attractive because a stable constant-current source is easy to construct and the total number of coulombs consumed in an electrolysis from the duration of electrolysis, $\tau$

$$Q = i_{app}\tau$$

e.g. coulometric determination of $Fe^{2+}$ by oxidation to $Fe^{3+}$ at Pt electrode in $H_2SO_4$ solution → <100% current efficiency → $Ce^{3+}$ addition, "coulometic titration"

$$Ce^{4+} + Fe^{2+} \rightarrow Ce^{3+} + Fe^{3+}$$

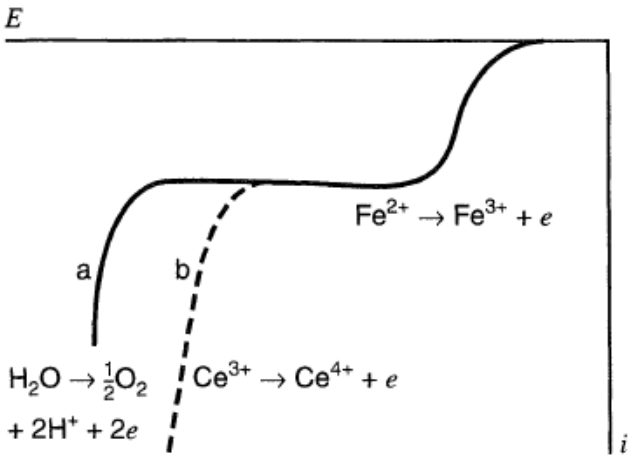


**Figure 11.4.4** Schematic *i-E* curves for $Fe^{2+}$ in 1 *M* $H_2SO_4$ in the absence (*curve a*) and in the presence (*curve b*) of excess $Ce^{3+}$.

galvanostat

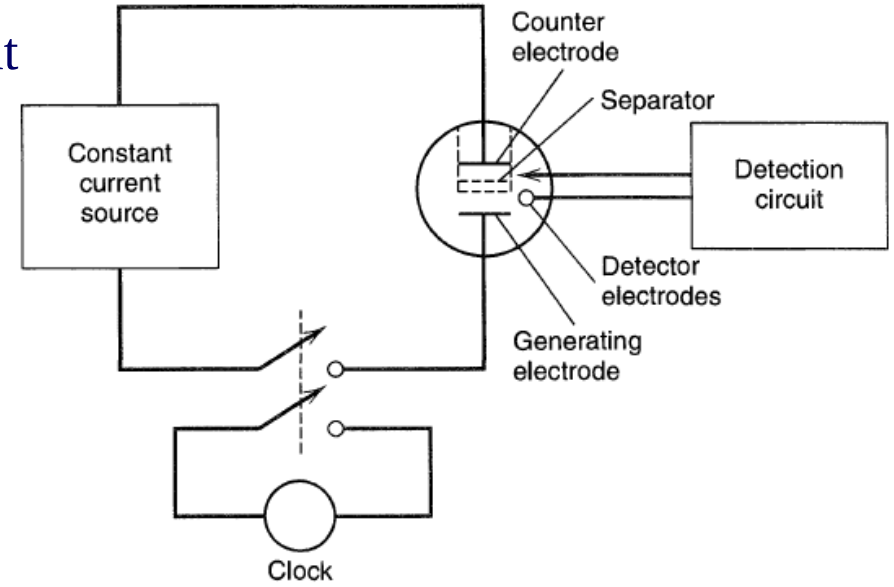


**Figure 11.4.5** Apparatus for coulometric titrations.

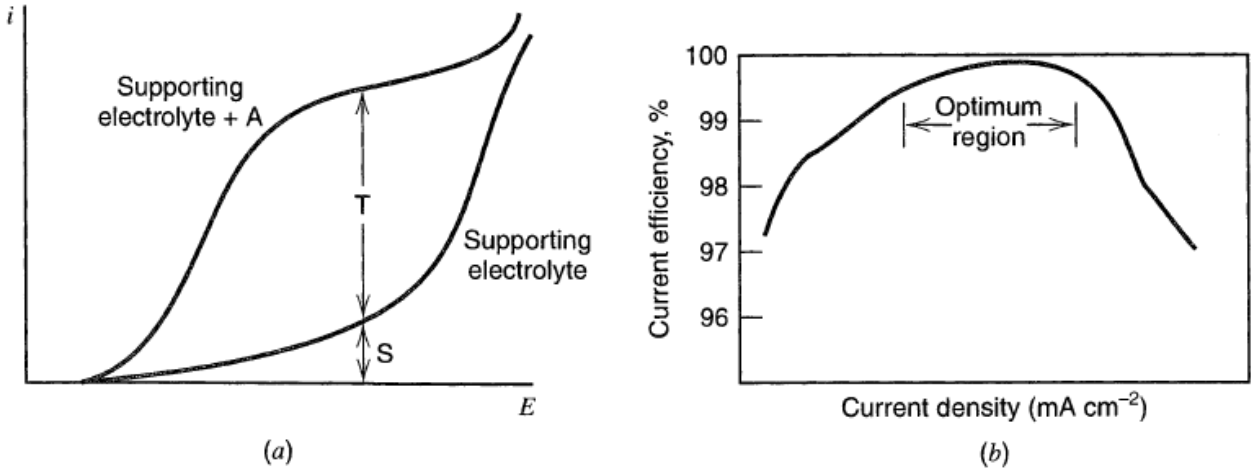


**Figure 11.4.6** (*a*) Use of *i*-*E* curves for estimating current efficiency at given potential and current density. (*b*) Typical plot of current efficiency as a function of current density for an electrogenerated titrant.

$$\text{Current efficiency} = \frac{100T}{T+S}$$

**TABLE 11.4.1 Typical Electrogenerated Titrants and Substances Determined by Coulometric Titration**

| Electrogenerated Titrant | Generating Electrode and Solution | Typical Substances Determined |
|---|---|---|
| | *Oxidants* | |
| Bromine | Pt/NaBr | As(III), U(IV), $NH_3$, olefins, phenols, $SO_2$, $H_2S$, Fe(II) |
| Iodine | Pt/KI | $H_2S$, $SO_2$, As(III), water (Karl Fischer), Sb(III) |
| Chlorine | Pt/NaCl | As(III), Fe(II), various organics |
| Cerium(IV) | $Pt/Ce_2(SO_4)_3$ | U(IV), Fe(II), Ti(III), $I^-$ |
| Manganese(III) | $Pt/MnSO_4$ | Fe(II), $H_2O_2$, Sb(III) |
| Silver(II) | $Pt/AgNO_3$ | Ce(III), V(IV), $H_2C_2O_4$ |
| | *Reductants* | |
| Iron(II) | $Pt/Fe_2(SO_4)_3$ | Mn(III), Cr(VI), V(V), Ce(IV), U(VI), Mo(VI) |
| Titanium(III) | $Pt/TiCl_4$ | Fe(III), V(V,VI), U(VI), Re(VIII), Ru(IV), Mo(VI) |
| Tin(II) | $Au/SnBr_4(NaBr)$ | $I_2$, $Br_2$, Pt(IV), Se(IV) |
| Copper(I) | Pt/Cu(II)(HCl) | Fe(III), Ir(IV), Au(III), Cr(VI), $IO_3^-$ |
| Uranium(V),(IV) | $Pt/UO_2SO_4$ | Cr(VI), Fe(III) |
| Chromium(II) | $Hg/CrCl_3(CaCl_2)$ | $O_2$,Cu(II) |
| | *Precipitation and Complexation Agents* | |
| Silver(I) | $Ag/HClO_4$ | Halide ions, $S^{2-}$, mercaptans |
| Mercury(I) | $Hg/NaClO_4$ | Halide ions, xanthate |
| EDTA | $Hg/HgNH_3Y^{2-a}$ | Metal ions |
| Cyanide | $Pt/Ag(CN)_2^-$ | Ni(II), Au(III,I), Ag(I) |
| | *Acids and Bases* | |
| Hydroxide ion | $Pt(-)Na_2SO_4$ | Acids, $CO_2$ |
| Hydrogen ion | $Pt(+)/Na_2SO_4$ | Bases, $CO_3^{2-}$, $NH_3$ |

[a] $Y^{4-}$ is ethylenediamine-tetra-acetate anion.

# 5. Electrometric end-point detection

# 6. Flow electrolysis

(1) Introduction

An alternative method of bulk electrolysis: flowing the solution to be electrolyzed continuously through a porous working electrode of large surface area → high efficiencies, rapid conversions, convenient where large amounts of solution are to be treated

Industrial applications: removal of metals from (waste) streams, electrosynthesis, separation, analysis

Flow electrolysis cell: a working electrode (screen of fine mesh metal or beds of conductive material (e.g. graphite, glassy carbon grains, metal shot, or powder), counter electrode, separators (porous glass, ceramics, ion-exchange membranes) → careful placement of electrodes to minimize iR drops

(2) Mathematical treatment

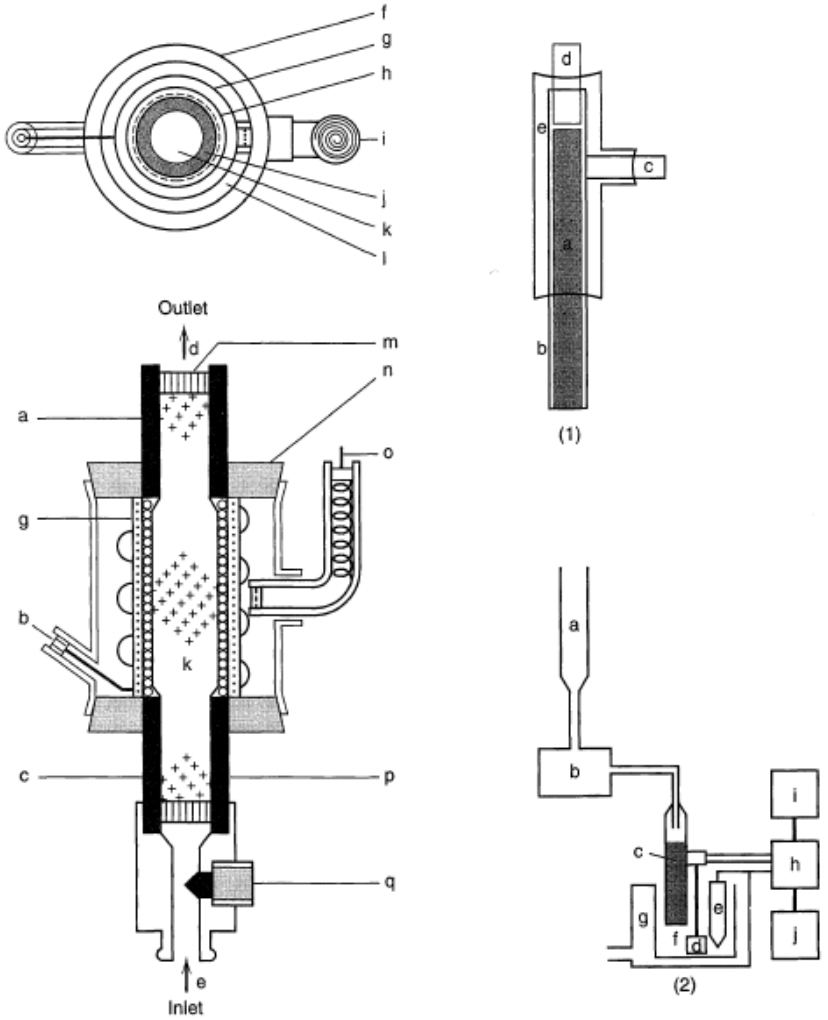


**Figure 11.6.1** Flow electrolytic cells. *Left:* Cell utilizing glassy carbon granule working electrode (k), silver auxiliary electrode (g), Ag/AgCl reference electrode (o, i) with porous glass separator (h). Other components are (a, c) lead for working electrode; (b) lead to auxiliary electrode; (d) solution outlet; (e) solution inlet; (f) glass or plastic tube; (j, p) porous carbon tube; (l) saturated KCl solution; (m) silicone rubber. [Reprinted with permission from T. Fujinaga and S. Kihara, *CRC Crit. Rev. Anal. Chem.*, **6**, 223 (1977). Copyright, CRC Press, Inc., Boca Raton, FL.] *Right:* Cell with Reticulated Vitreous Carbon (RVC™), a conductive foam-type material available in several porosities. (*1*) (a) RVC cylinder, (b) heat-shrink tubing, (c) graphite rod sidearm, (d) glass tube, (e) glass and epoxy support. (2) Schematic diagram of complete apparatus. (a) Solution reservoir, (b) pump, (c) RVC electrode, (d) platinum electrode, (e) SCE reference electrode, (f) downstream reservoir, (g) runover collector, (h) potentiostat, (i) recorder, (j) digital voltmeter. [Reprinted with permission from A. N. Strohl and D. J. Curran, *Anal. Chem.*, **51**, 353 (1979). Copyright 1979, American Chemical Society.]

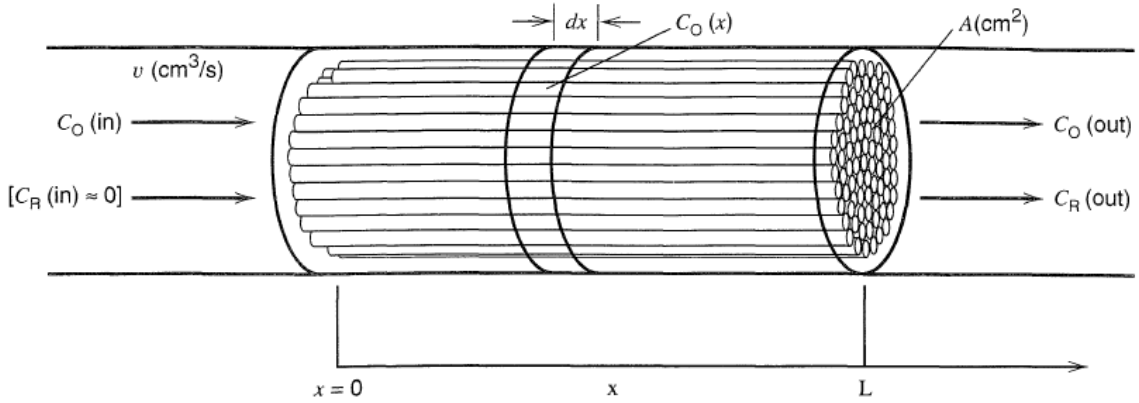


**Figure 11.6.2** Schematic diagram of the working electrode of a flow electrolysis cell.

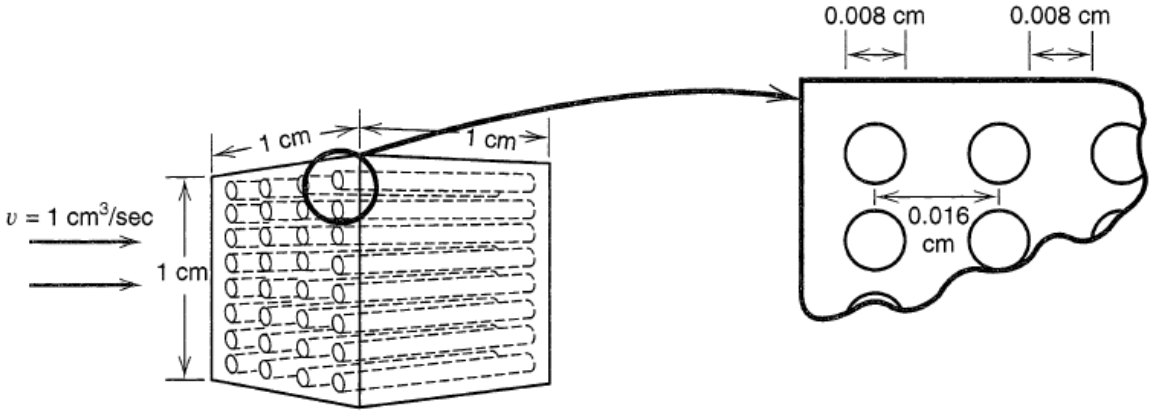


**Figure 11.6.3** Ideal porous electrode illustrating calculation of the specific area, $s$, and porosity, $\varepsilon$. Consider the electrode as a cube $1 \times 1 \times 1$ (cm), containing straight pores, each 0.008 cm in diameter, spaced at centers 0.016 cm apart. The total number of pores, $N$, on a 1-$cm^2$ face is ~3900; the internal area of each pore is $2\pi rL = \pi(0.008\text{ cm})(1\text{ cm}) = 0.025\text{ cm}^2$; the total internal electrode area is $a = (3900)(0.025\text{ cm}^2) = 98\text{ cm}^2$; the total electrode volume is 1 $cm^3$; the specific area is $s = 98\text{ cm}^2/1\text{ cm}^3 = 98\text{ cm}^{-1}$; the facial area of each pore is $\pi r^2 = 5.0 \times 10^{-5}\text{ cm}^2$; the total open area on face is $a_p = (3900)(5.0 \times 10^{-5}\text{ cm}^2) = 0.2\text{ cm}^2$; the porosity is $\varepsilon = 0.2\text{ cm}^2/1\text{ cm}^2 = 0.2$. If the volumetric flow rate is $v = 1\text{ cm}^3/\text{s}$, the linear flow velocity is $U = 1\text{ cm}^3/\text{s}\ /1\text{ cm}^2 = 1\text{ cm/s}$, and the interstitial velocity is $W = 1\text{ cm/s}\ /0.2 = 5\text{ cm/s}$.

(3) Dual-electrode flow cells

Flow cells that incorporate two working electrodes in the flow channel → convective flow carries material from the first working electrode to the second

cf. rotating ring-disk electrode (RRDE)

e.g.
1st electrode: the generator ($O + ne \rightarrow R$), 2nd electrode: the collector ($R \rightarrow O + ne$)
1st electrode: plutonium oxidation to Pu(IV), 2nd electrode: $Pu(IV) + e \rightarrow Pu(III)$)

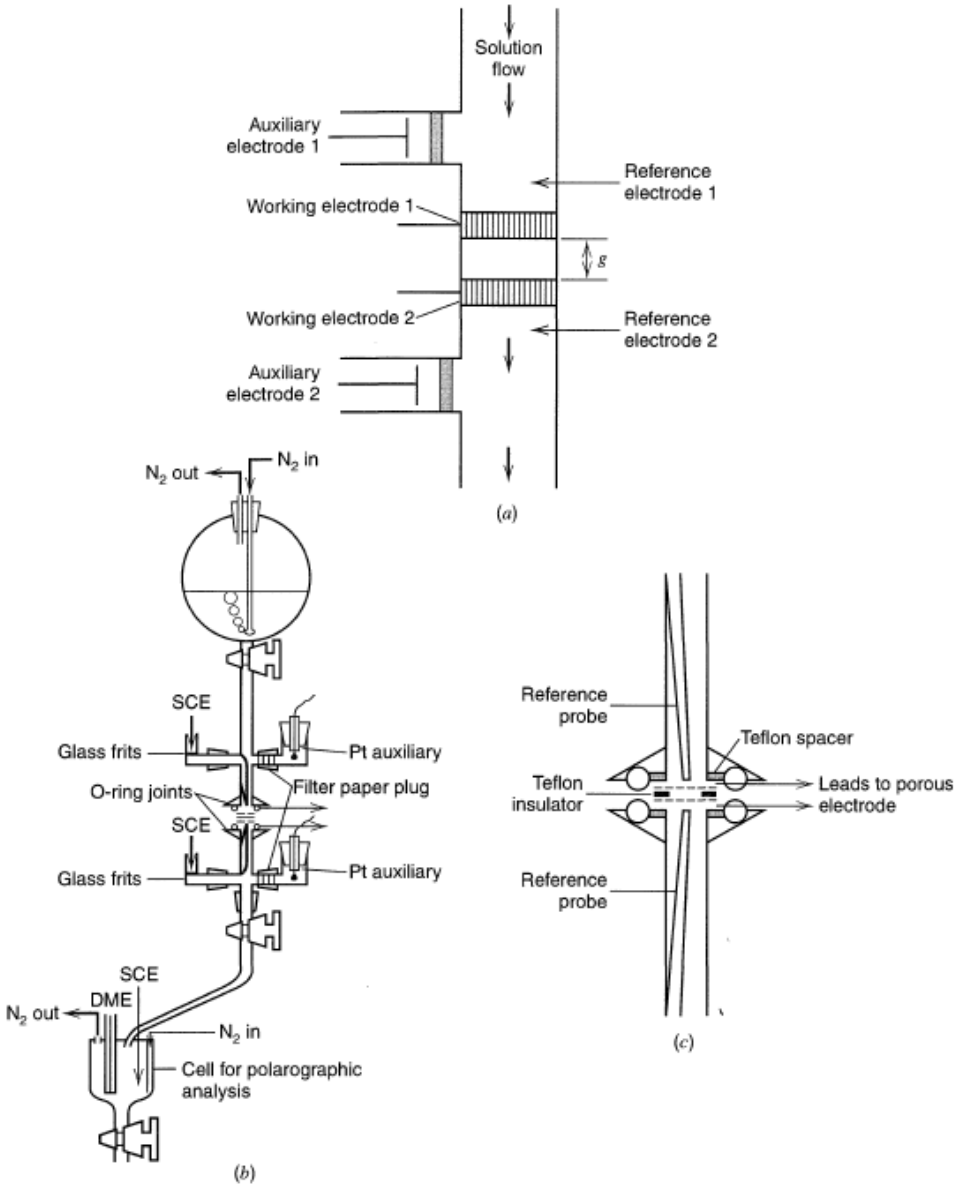


**Figure 11.6.4** (*a*) Schematic representation of a dual-electrode flow cell. (*b*) Actual complete dual-electrode flow cell assembly. Solution flows by gravity from upper reservoir. For greater clarity, the "O-ring joint" portion of the cell with the dual working electrodes is shown in exploded form. A close-up view of this portion with the porous silver electrodes is shown in (*c*). [From J. V. Kenkel and A. J. Bard, *J. Electroanal. Chem.*, **54**, 47 (1974), with permission.]

# (4) Electrochemical detectors for liquid chromatography (EDLC)

Applications of flow cells: detectors for liquid chromatography, capillary zone electrophoresis(CZE) → convective flow carries material from the first working electrode to the second

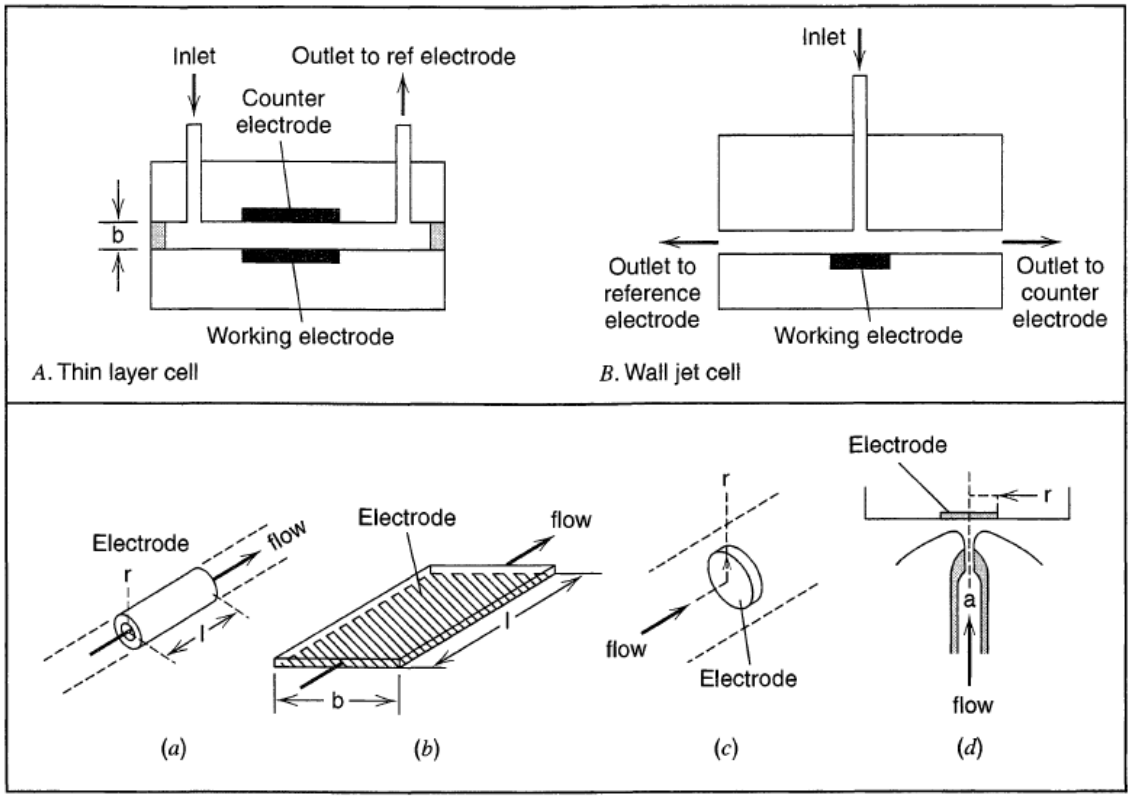


**Figure 11.6.5** Typical cell arrangements and electrode geometries for electrochemical flow cells. *Top*: (*A*) Thin-layer cell. (*B*) Wall-jet cell. *Bottom*: Various electrode geometries: (a) tubular electrode; (b) planar electrode with parallel flow; (c) planar electrode with perpendicular flow; (d) wall-jet electrode. [Reprinted from H. Gunasingham and B. Fleet, *Electroanal. Chem.*, **16**, 89 (1989), by courtesy of Marcel Dekker, Inc.]

**TABLE 11.6.1 Limiting Currents for Different Cell Geometries**[a]

| Electrode Geometry | Limiting Current Equation[b] |
|---|---|
| Tubular | $i = 1.61nFC(DA/r)^{2/3}v^{1/3}$ |
| Planar, parallel flow in channel | $i = 1.47nFC(DA/b)^{2/3}v^{1/3}$ |
| Planar, perpendicular flow | $i = 0.903nFCD^{2/3}\nu^{-1/6}A^{3/4}U^{1/2}$ |
| Wall jet | $i = 0.898nFCD^{2/3}\nu^{-5/12}a^{-1/2}A^{3/8}v^{3/4}$ |

[a]Adapted from J. M. Elbicki, D. M. Morgan, and S. G. Weber, *Anal. Chem.*, **56**, 978 (1984). See Figure 11.6.5 for illustration of types.

[b]$a$ = diameter of jet inlet, $A$ = electrode area, $b$ = channel height, $C$ = concentration, $D$ = diffusion coefficient, $\nu$ = kinematic viscosity, $r$ = radius of tubular electrode, $v$ = average volume flow rate ($cm^3/s$), $U$ = flow velocity (cm/s).

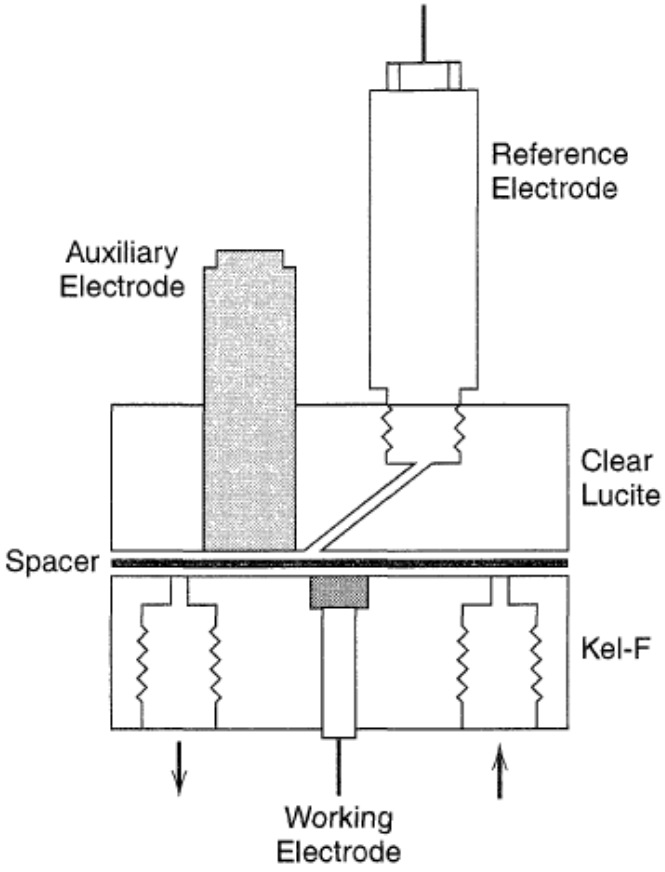


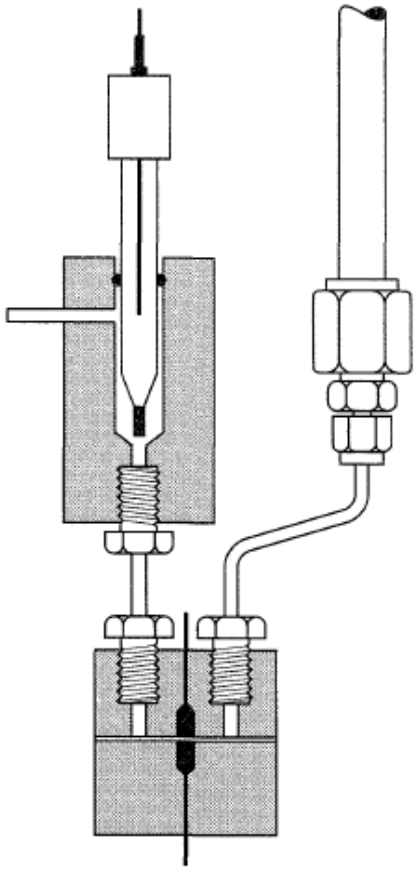

**Figure 11.6.6** Thin-layer LC detector cells. *Left*: Cell with auxiliary and reference electrodes in thin-layer portion downstream from working electrode. [Reprinted from J. A. Wise, W. R. Heineman and P. T. Kissinger, *Anal. Chim. Acta*, **172**, 1 (1985), with permission from Elsevier Science.] *Right*: Cell with facing working and auxiliary electrodes and reference electrode downstream in flow channel. [Courtesy of Bioanalytical Systems, Inc.]

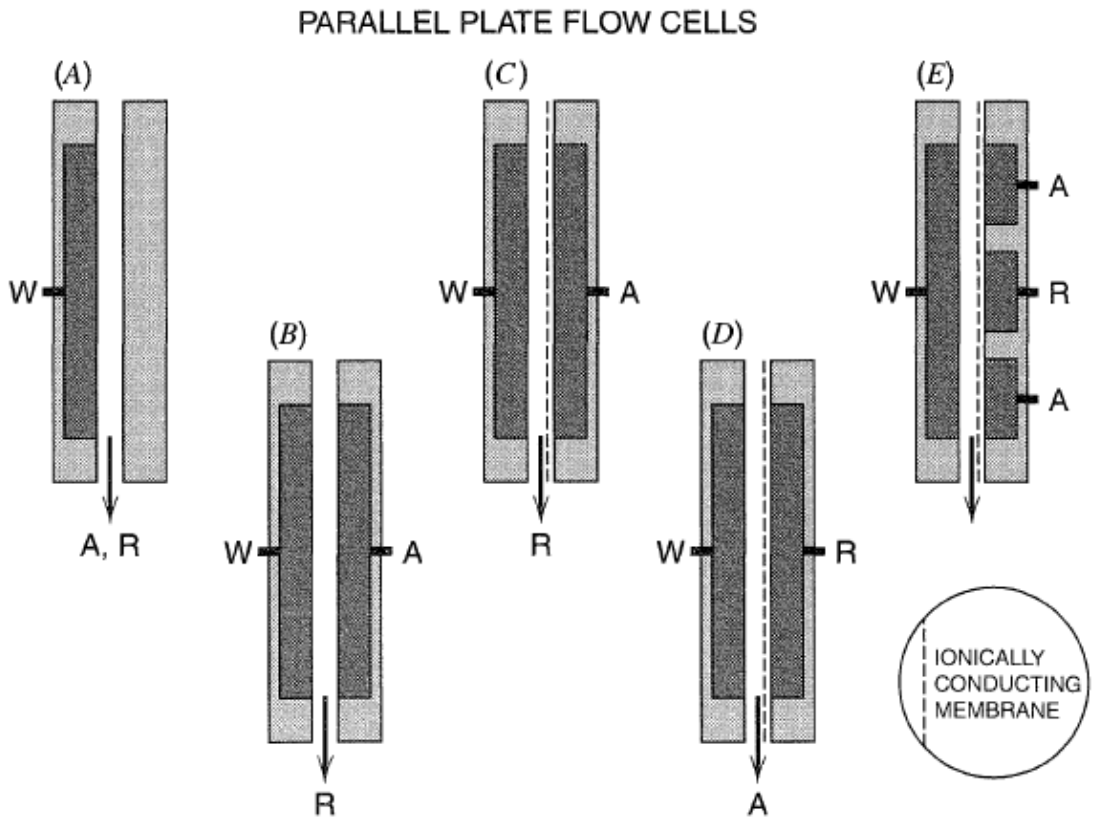


**Figure 11.6.7** Different geometries for thin-layer electrochemical detector cells involving different placements of the working (W), auxiliary (A) and reference (R) electrodes. [Reprinted from S. M. Lunte, C. E. Lunte, and P. T. Kissinger, in "Laboratory Techniques in Electroanalytical Chemistry," 2nd ed., P. T. Kissinger and W. R. Heineman, Eds., Marcel Dekker, New York, 1996, by courtesy of Marcel Dekker, Inc.]

The simplest electrochemical technique for LC is amperometry: working electrode potential is fixed → detect oxidized or reduced current flow as they pass from the column

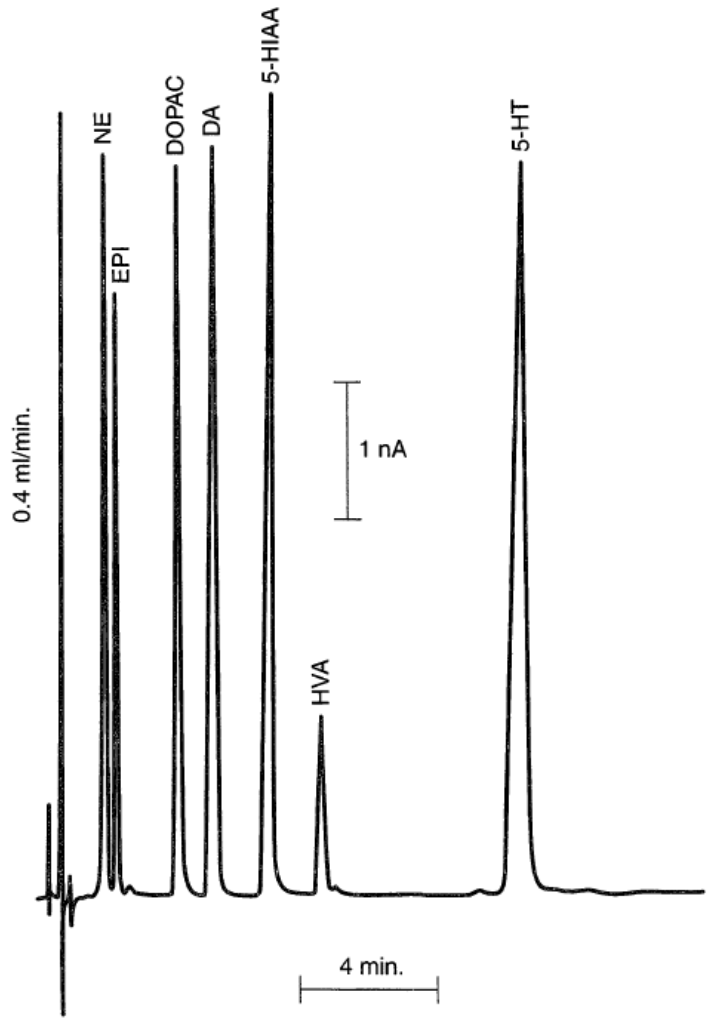


**Figure 11.6.8** Liquid chromatographic separation of tryptophan and tyrosine metabolites using amperometric detection with a glassy carbon working electrode at 0.65 V *vs.* Ag/AgCl in a thin-layer cell. NE, norepinephrine; EPI, epinephrine; DOPAC, 3,4-hydroxyphenylacetic acid; DA, dopamine; 5-HIAA, 5-hydroxyindole-3-acetic acid; HVA, homovanillic acid; 5-HT, serotonin (5-hydroxytryptamine). [From T. Huang and P. T. Kissinger, *Curr. Separations*, **14**, 114 (1996), with permission.]

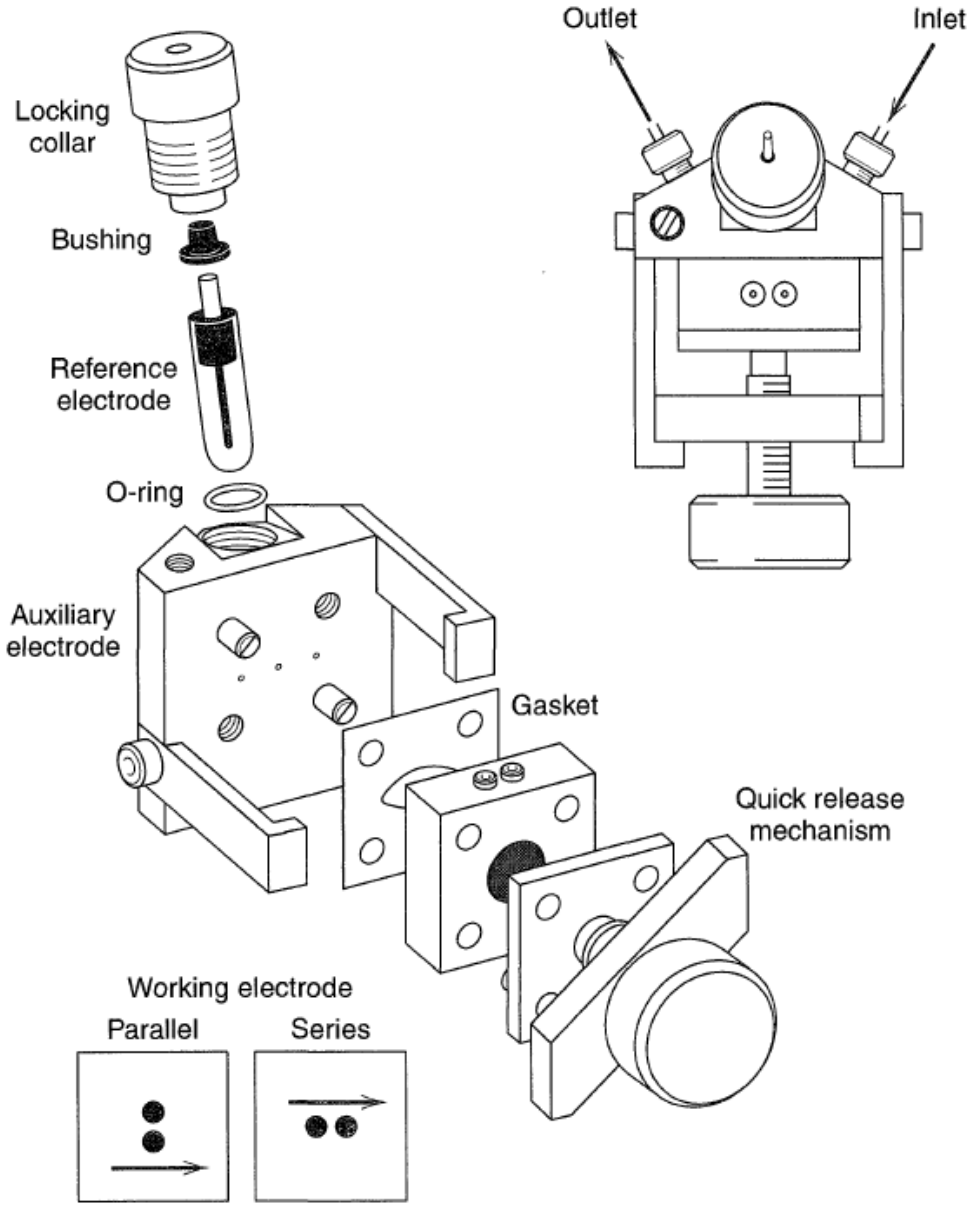


**Figure 11.6.9** Cell with dual working electrodes and cross-flow design [Reprinted from S. M. Lunte, C. E. Lunte, and P. T. Kissinger, in "Laboratory Techniques in Electroanalytical Chemistry," 2nd ed., P. T. Kissinger and W. R. Heineman, Eds., Marcel Dekker, New York, 1996, by courtesy of Marcel Dekker, Inc.]

# 7. Thin-layer electrochemistry

(1) Introduction

An alternative method of bulk electrolysis conditions and a large A/V ratio: decreasing V (a very small solution volume is confined to a thin layer) → cell thickness, *l*, is smaller than the diffusion layer thickness, $l << (2Dt)^{1/2}$. Mass transfer within the cell can be neglected

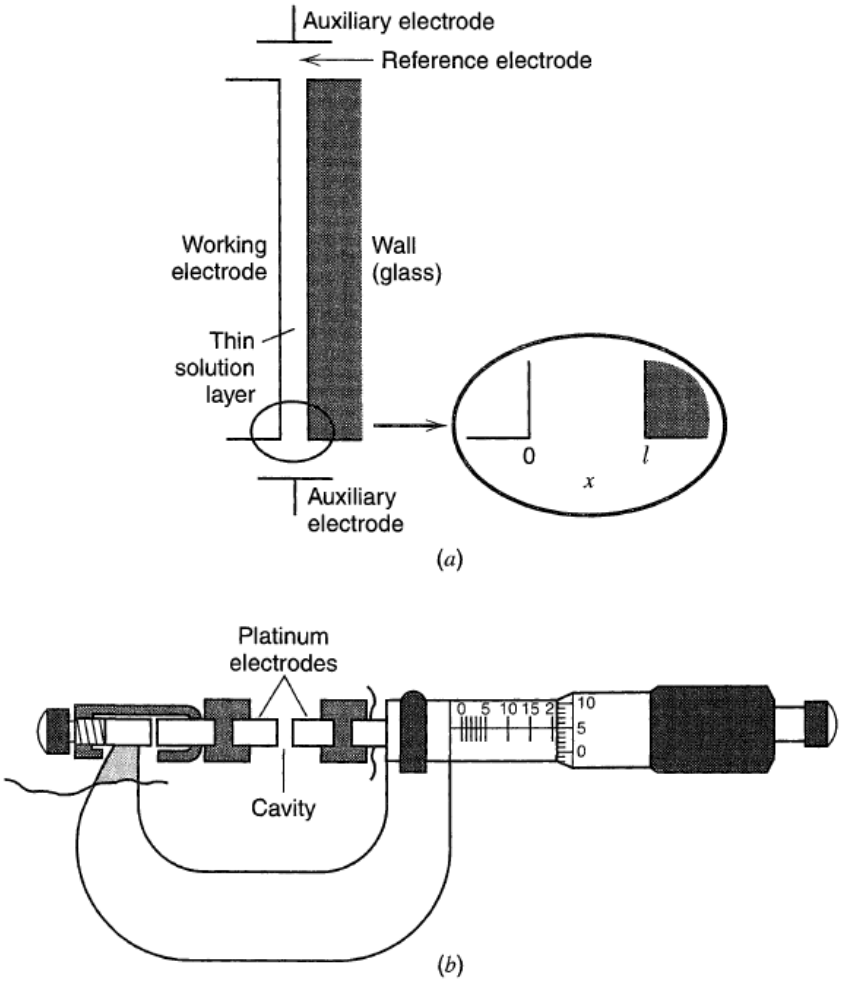


**Figure 11.7.1** (*a*) Schematic diagram of a single-electrode thin-layer cell. (*b*) Micrometer, twin-electrode thin-layer cell with adjustable solution layer thickness.

(*continued*

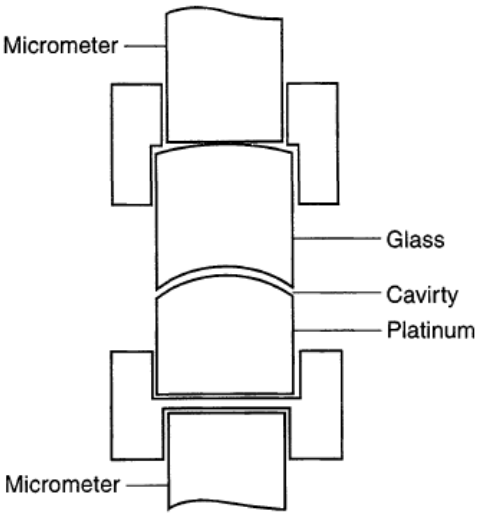


(*c*)

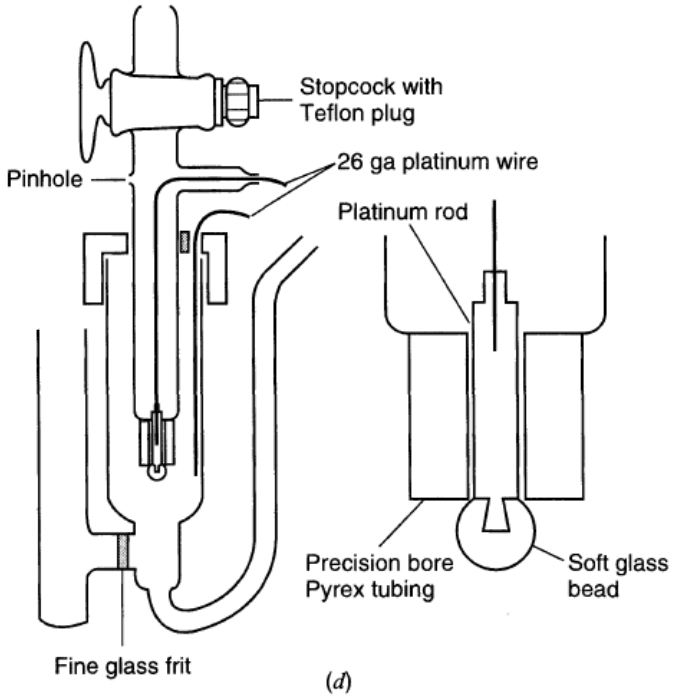


(*d*)

**Figure 11.7.1** Continued (*c*) Close-up of electrode portion for single-electrode configuration of (*b*). (*d*) Capillary-wire single-electrode thin-layer electrode. The solution layer is contained in the small space between the metal rod and the inner surface of the precision-bore capillary. The layer thickness is typically $2.5 \times 10^{-3}$ cm. The metal rod may be positioned within the capillary to a high degree of concentricity by machining three small flanges onto the surface of the rod near each end. Highly reproducible rinsing and filling are accomplished by alternately applying and releasing nitrogen pressure with the stopcock. [From A. T. Hubbard and F. C. Anson, *Electroanal. Chem.*, **4**, 129 (1970), by courtesy of Marcel Dekker, Inc.]

## (2) Potential step (coulometric) methods

Potential step $E_1$ (no current flows) to $E_2$ ($O + ne \rightarrow R$ complete and no O at the electrode surface) → i-t behavior & the concentration profile

$$\frac{\partial C_O(x, t)}{\partial t} = D_O\left(\frac{\partial^2 C_O(x, t)}{\partial x^2}\right)$$

with the boundary conditions

$$C_O(x, 0) = C_O^* \qquad t = 0; 0 \le x \le l$$

$$C_O(0, t) = C_O(l, t) = 0 \qquad t > 0$$

Solution

$$C_O(x, t) = \frac{4C_O^*}{\pi} \sum_{m=1}^{\infty} \left(\frac{1}{2m - 1}\right) \exp\left[\frac{-(2m - 1)^2 \pi^2 D_O t}{l^2}\right] \sin \frac{(2m - 1)\pi x}{l}$$

Concentration profile (Fig. 11.7.2a)

$$C_O(x, t) \approx \frac{4C_O^*}{\pi} \exp\left(\frac{-\pi^2 D_O t}{l^2}\right) \sin \frac{\pi x}{l}$$

$$i(t) = nFAD_O\left[\frac{\partial C_O(x,t)}{\partial x}\right]_{x=0}$$

$$\boxed{i(t) = \frac{4nFAD_O C_O^*}{l}\sum_{m=1}^{\infty}\exp\left[\frac{-(2m-1)^2\pi^2 D_O t}{l^2}\right]}$$

$$i(t) \approx i(0)\exp(-pt) \qquad \text{(11.7.8) (same as (11.3.7)}$$

with

$$p = \frac{\pi^2 D_O}{l^2} = \frac{\pi^2 D_O A}{Vl} = \frac{m_O A}{V}$$

$$m_O = \frac{\pi^2 D_O}{l} \quad \text{and} \quad i(0) = \frac{4nFAC_O^* m_O}{\pi^2}$$

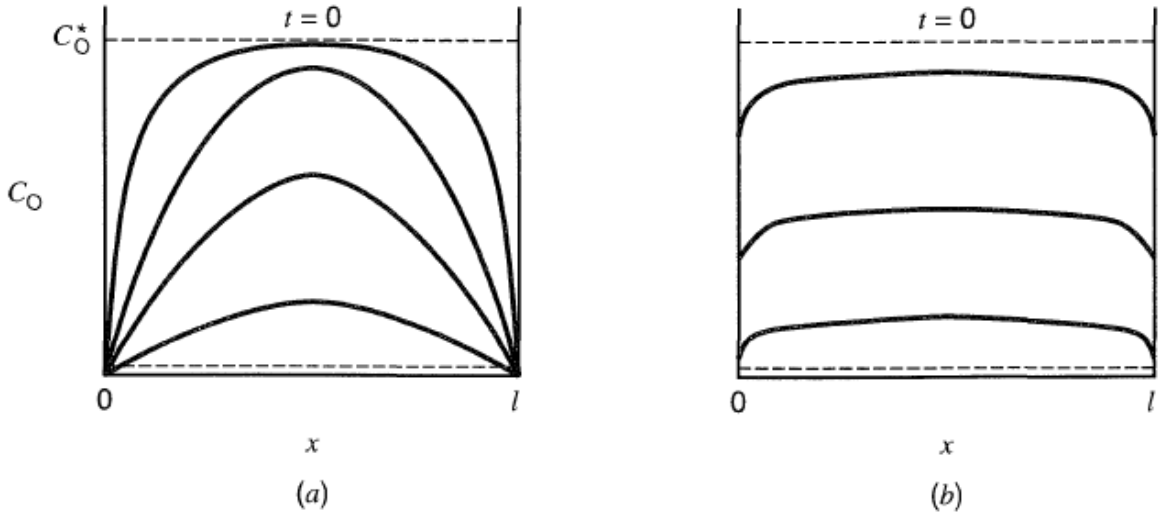


**Figure 11.7.2**
Concentration of O during reduction of O in twin-electrode thin-layer cell. (*a*) Actual profiles. (*b*) Neglecting mass transfer in cell.

The total charge passed by the electrolytic reaction

$$Q(t) = nFVC_O^*\left\{1 - \frac{8}{\pi^2}\sum_{m=1}^{\infty}\left(\frac{1}{2m-1}\right)^2 \exp\left[\frac{-(2m-1)^2\pi^2 D_O t}{l^2}\right]\right\}$$

$$Q(t) \approx nFVC_O^*\left(1 - \frac{8}{\pi^2}e^{-pt}\right) \qquad \text{(later times)}$$

$$Q(t \to \infty) = nFVC_O^* = nFN_O \qquad (11.7.11)\ \text{(same as (11.3.11)}$$

(3) Potential sweep methods

Potential sweep from $E_i$ (no reaction occurs) toward negative values. The concentration of O and R can be considered uniform ($C_O(x,t) = C_O(t)$ and $C_R(x, t) = C_R(t)$ for $0 \le x \le l$)

$$i = -nFV\left[\frac{dC_O(t)}{dt}\right] \qquad (11.7.12)$$

For a nernstian reaction

$$E = E^{0'} + \frac{RT}{nF}\ln\frac{C_O(t)}{C_R(t)}$$

$$C_O^* = C_O(t) + C_R(t)$$

Combination of these two equation

$$C_O(t) = C_O^*\left\{1 - \left[1 + \exp\left(\frac{nF}{RT}(E - E^{0'})\right)\right]^{-1}\right\} \qquad (11.7.15)$$

Differentiation of (11.7.5) and substitution into (11.7.12) with the sweep rate,v (= -(dE/dt))

$$i = \frac{n^2F^2vVC_O^*}{RT}\frac{\exp\left[\left(\frac{nF}{RT}\right)(E - E^{0'})\right]}{\left\{1 + \exp\left[\left(\frac{nF}{RT}\right)(E - E^{0'})\right]\right\}^2}$$

The peak current occurs at E = $E^{0'}$

$$i_p = \frac{n^2 F^2 v V C_O^*}{4RT} \qquad (11.7.15)$$

A typical scan voltammogram in a thin-layer cell: the peak current is directly proportional to v, but the total charge under the i-E curve, given by (11.7.11), is independent of v

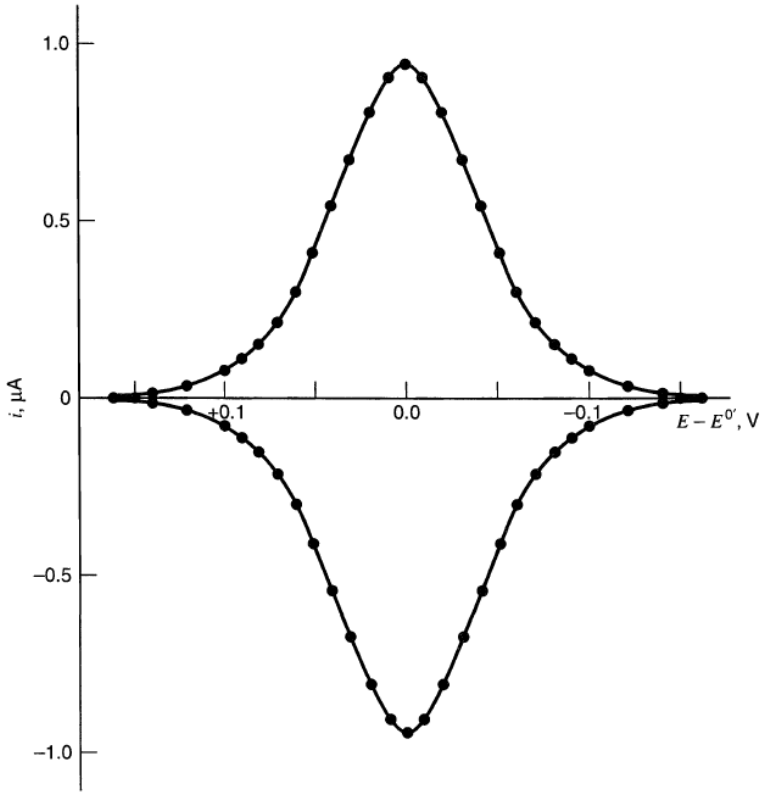


**Figure 11.7.3** Cyclic current-potential curve for a nernstian reaction with $n = 1$, $V = 1.0\ \mu L$, $|v| = 1$ mV/s, $C_O^* = 1.0$ m$M$, $T = 298$ K. [From A. T. Hubbard and F. C. Anson, *Electroanal. Chem.*, **4**, 129 (1970), by courtesy of Marcel Dekker, Inc.]

For a totally irreversible one-step, one-electron reaction

$$\frac{i}{FA} = k_f C_O(t) \qquad (11.7.19)$$

where $k_f = k^0 \exp(-\alpha F/RT)(E - E^{0'})$

By combination (11.7.19) with (11.7.12)

$$\frac{dC_O(t)}{dt} = -\left[\frac{Ak_f(t)}{V}\right] C_O(t) \qquad (11.7.20)$$

In a potential sweep experiment, $E(t) = E_i - vt$, $f = F/RT$

$$k_f(t) = k^0 \exp[-\alpha f(E_i - E^{0'})] \exp(\alpha f v t) \qquad (11.7.21)$$

By substitution of (11.7.21) into (11.7.20 and integration between t = 0 ($C_O = C_O^*$) and t ($C_O = C_O(t)$) under the conditions that $k^0 \exp(-\alpha f)(E - E^{0'}) \rightarrow 0$ (i.e. an initial potential well positive of $E^{0'}$)

$$C_O(E) = C_O^* \exp\left(\frac{-RT}{\alpha F}\frac{Ak_f}{Vv}\right)$$

$$i(E) = FAk_f C_O^* \exp\left(\frac{-RT}{\alpha F}\frac{Ak_f}{Vv}\right)$$

Substituting $k_f$

$$i(E) = FAk^0C_O^* \exp\left\{-\alpha f(E - E^{0'}) - \frac{Ak^0}{\alpha f V v} \exp[-\alpha f(E - E^{0'})]\right\} \qquad (11.7.24)$$

Typical i-E curves for totally irreversible reduction of O to R in a thin-layer cell

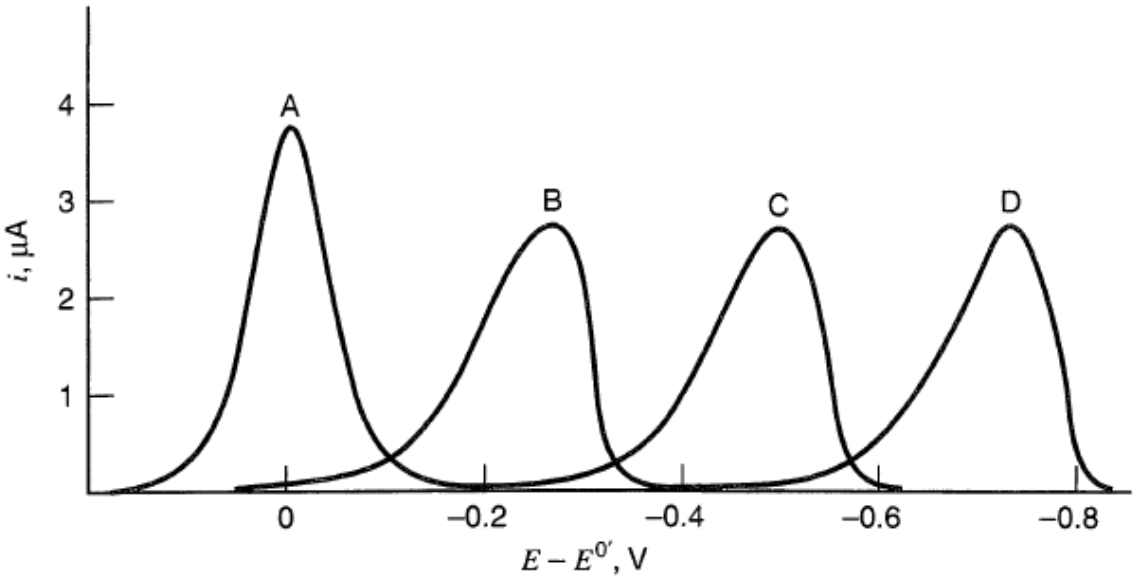


**Figure 11.7.4** Theoretical cathodic current-potential curves for one-step, one-electron irreversible reactions according to (11.7.24) for several values of $k^0$. *Curve A*: reversible reaction (shown for comparison). *Curve B*: $k^0 = 10^{-6}$. *Curve C*: $k^0 = 10^{-8}$. *Curve D*: $k^0 = 10^{-10}$ cm/s. The values assumed in making the plots were $|v| = 2$ mV/s, $A = 0.5$ cm$^2$, $C_O^* = 1.0$ m$M$, $\alpha = 0.5$, $V = 2.0$ $\mu$L. [From A. T. Hubbard, *J. Electroanal. Chem.*, **22**, 165 (1969), with permission.]

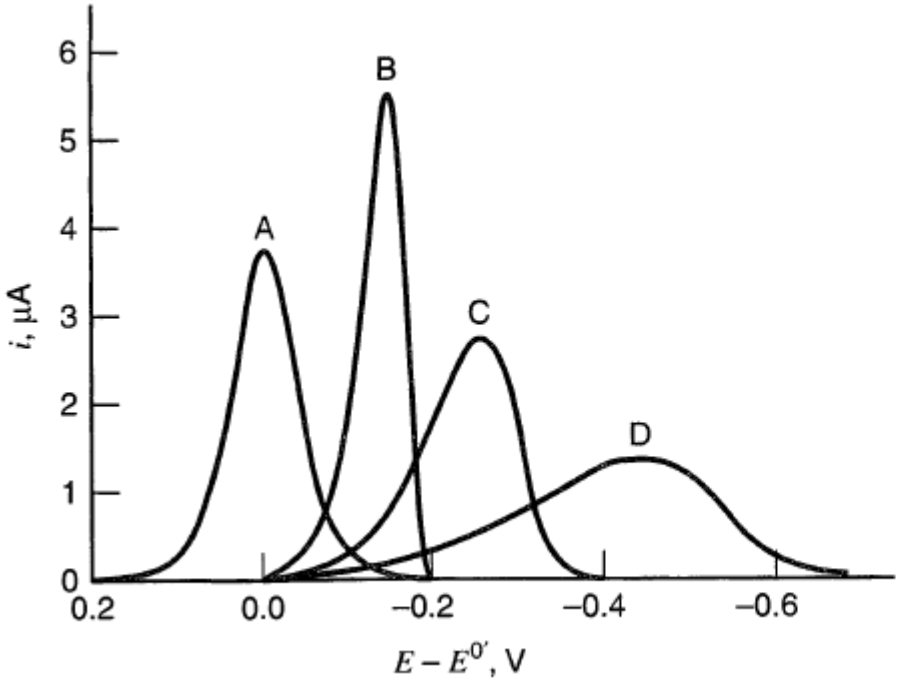


**Figure 11.7.5** Theoretical cathodic current-potential curves for one-step, one-electron irreversible reactions for several values of $\alpha$. *Curve A*: reversible reaction. *Curve B*: $\alpha = 0.75$, $k^0 = 10^{-6}$ cm/s. *Curve C*: $\alpha = 0.5$, $k^0 = 10^{-6}$ cm/s. *Curve D*: $\alpha = 0.25$, $k^0 = 10^{-6}$ cm/s. The values assumed in making the graphs were: $|v| = 2$ mV/s, $A = 0.5$ cm$^2$, $C_O^* = 1.0$ m$M$, $V = 2.0$ $\mu$L. [From A. T. Hubbard, *J. Electroanal. Chem.*, **22**, 165 (1969), with permission.]

Peak potential (by differentiating (11.7.24))

$$E_{pc} = E^{0'} + \frac{RT}{\alpha F} \ln\left(\frac{ARTk^0}{\alpha F V v}\right) \qquad (11.7.25)$$

Peak current is still proportional to v and $C_O^*$

$$i_{pc} = \frac{\alpha F^2 V v C_O^*}{2.718RT} \qquad (11.7.26)$$

# 8. Stripping analysis

## (1) Introduction

Stripping analysis is an analytical method that utilizes a bulk electrolysis step (preelectrolysis) to preconcentrate a substance from solution into the small volume of a mercury electrode or onto the surface of an electrode

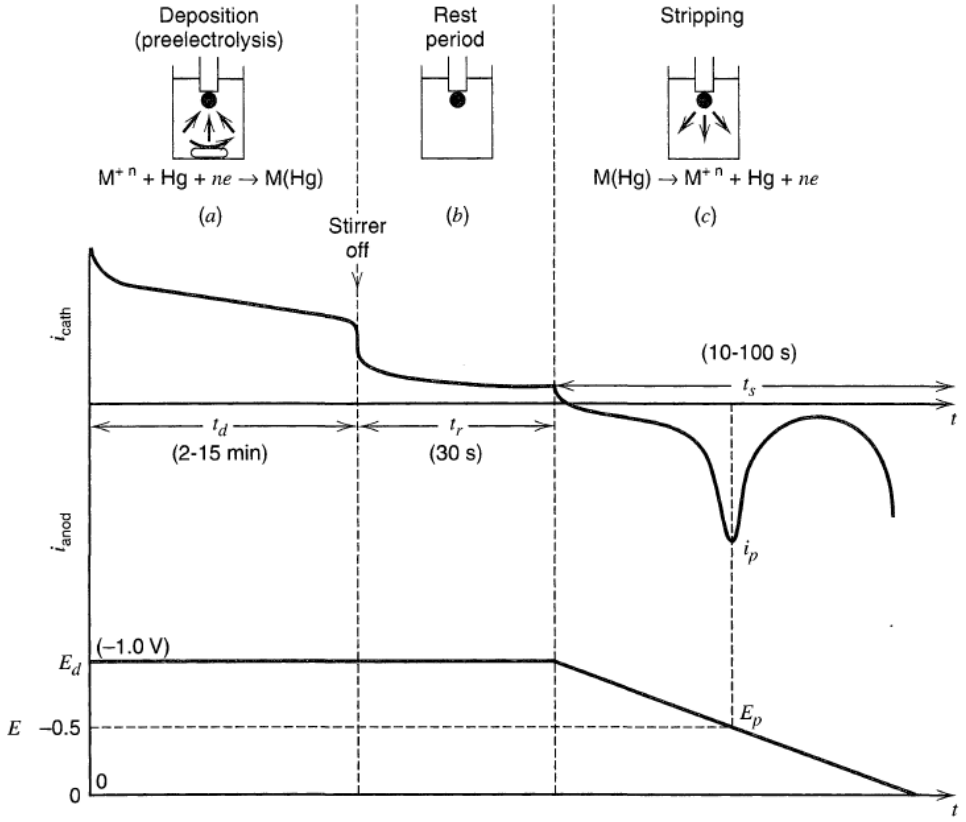


**Figure 11.8.1** Principle of anodic stripping. Values shown are typical ones used; potentials and $E_p$ are typical of $Cu^{2+}$ analysis. (*a*) Preelectrolysis at $E_d$; stirred solution. (*b*) Rest period; stirrer off. (*c*) Anodic scan ($v$ = 10–100 mV/s). [Adapted from E. Barendrecht, *Electroanal. Chem.*, **2**, 53 (1967), by courtesy of Marcel Dekker, Inc.]

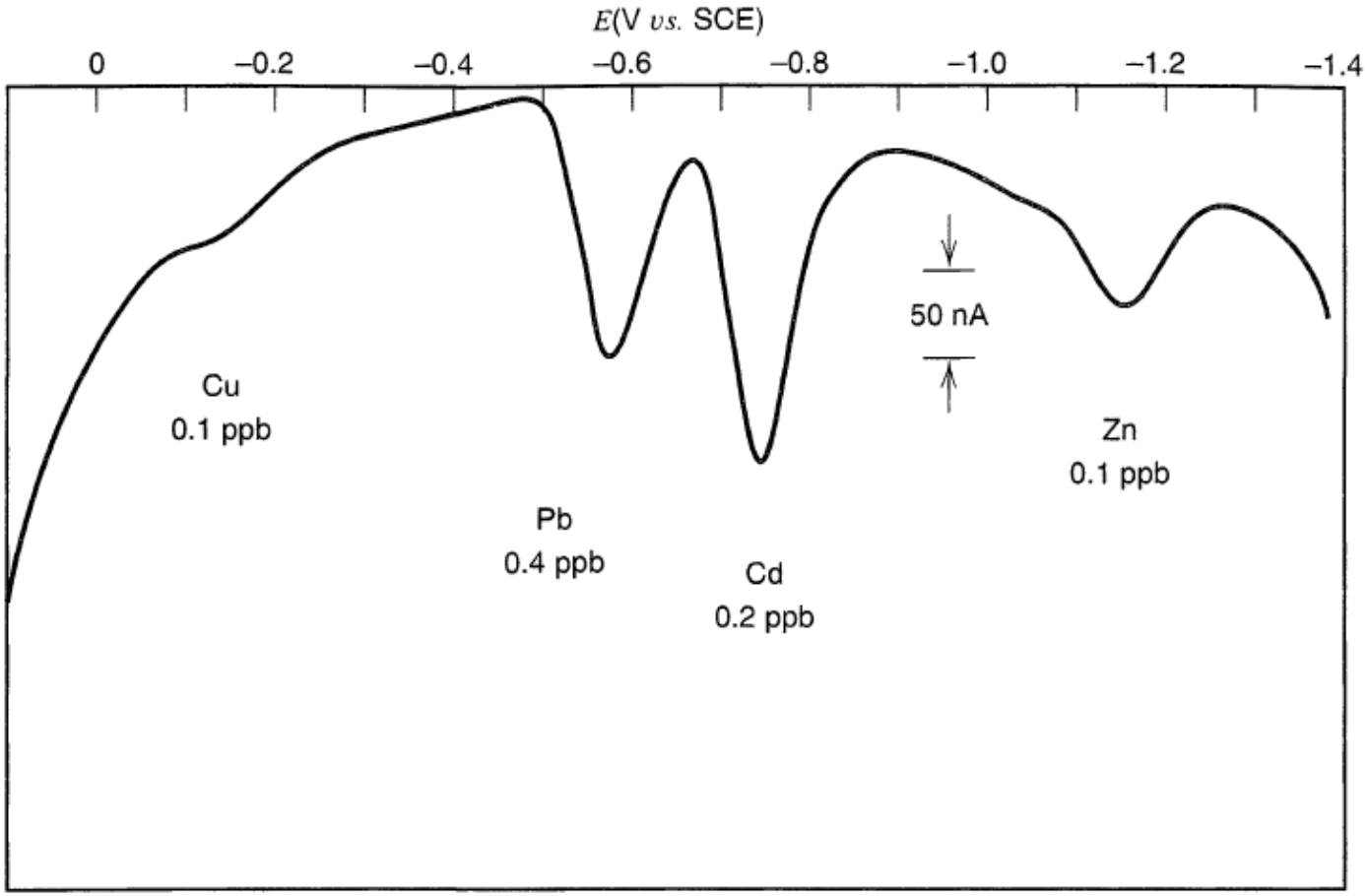


**Figure 11.8.5** Anodic stripping analysis of a solution containing $2 \times 10^{-9}$ *M* Zn, Cd, Pb, and Cu at an MFE (mercury-plated, wax-impregnated graphite electrode). Stripping carried out by differential pulse voltammetry.

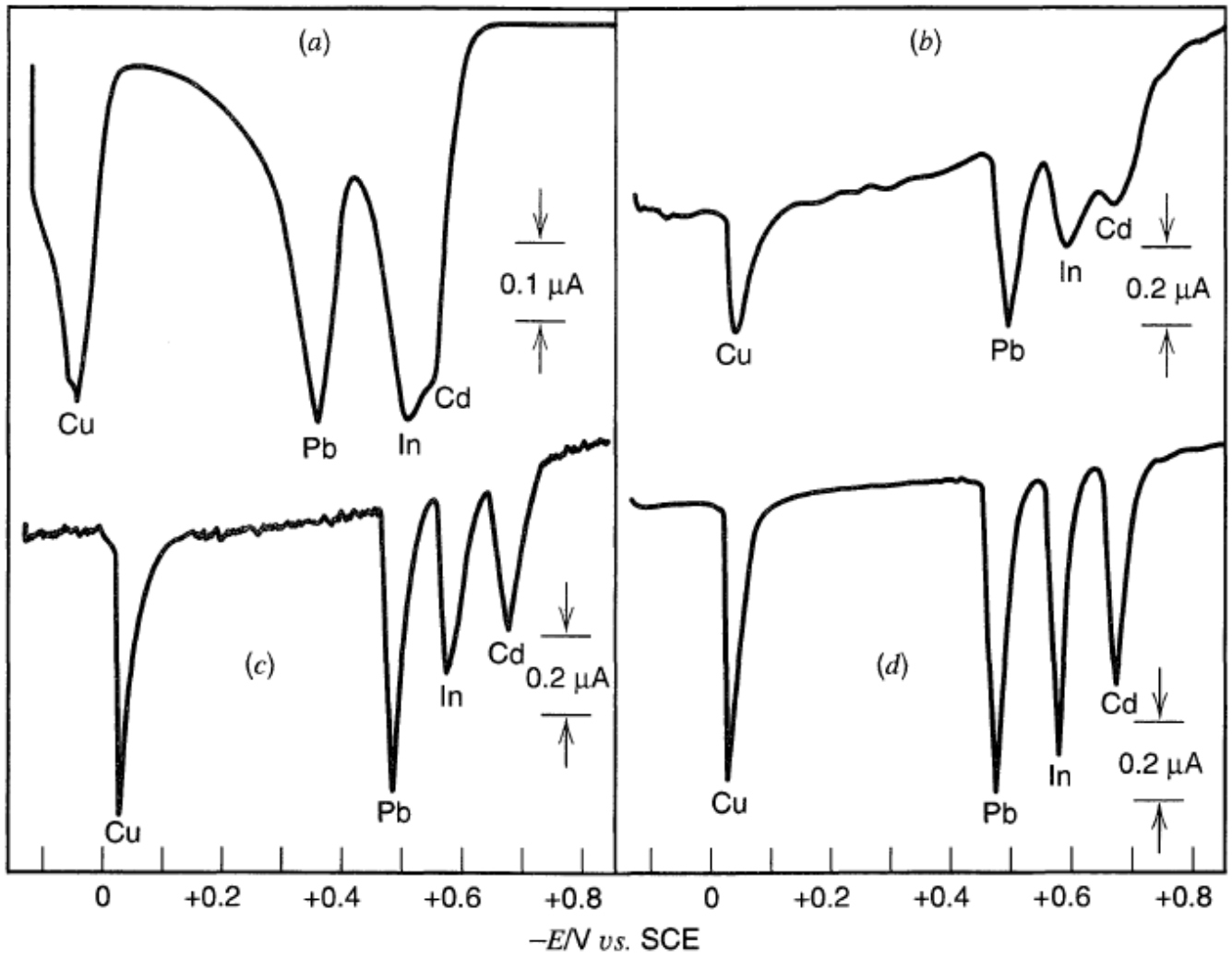


**Figure 11.8.6** Stripping curves for $2 \times 10^{-7}$ *M* $Cd^{2+}$, $In^{3+}$, $Pb^{2+}$, and $Cu^{2+}$ in 0.1 *M* $KNO_3$. $|v| = 5$ mV/s. (*a*) HMDE, $t_d = 30$ min. (*b*) Pyrolytic graphite, $t_d = 5$ min. (*c*) Unpolished glassy carbon, $t_d = 5$ min. (*d*) Polished glassy carbon, $t_d = 5$ min. For (*b*) to (*d*), $\omega/2\pi = 2000$ rpm and $Hg^{2+}$ was added at $2 \times 10^{-5}$ *M*. [From T. M. Florence, *J. Electroanal. Chem.*, **27**, 273 (1970), with permission.]